DNA-Based Oscillator Reactions

John Reif

DNA as a universal substrate for chemical kinetics

David Soloveichik, Georg Seelig, and Erik Winfree,

PNAS, vol. 107 no. 12, 5393–5398, 2010
www.pnas.org/cgi/doi/10.1073/pnas.0909380107

(Used DNA Strand Displacement Reactions to Create Oscillators)
(Simulations only)

Lotka–Volterra Chemical Oscillator:

X_1 = prey (reproduces)

X_2 = predator (consumes prey)

(A) The formal chemical reaction system to be implemented with original (unscaled) and scaled rate constants.

Initial concentrations of X_1 and X_2 are 2 and 1 unscaled and 20 and 10 nM scaled.

A Ideal chemical reactions

$$1:\ X_1 + X_2 \xrightarrow{k_1} 2X_2$$

$$2:\ X_1 \xrightarrow{k_2} 2X_1$$

$$3:\ X_2 \xrightarrow{k_3} \emptyset$$

	unscaled	scaled
k_1	1.5	$5{\cdot}10^5$ /M/s
k_2	1	1/300 /s
k_3	1	1/300 /s

(C) Plot of the concentrations of:

- **X_1 (Red curve) and**
- **X_2 (Green curve)**

Plot for the ideal system (Dashed line)

Corresponding DNA species: (Solid line).

C Simulation of ideal and DNA reactions

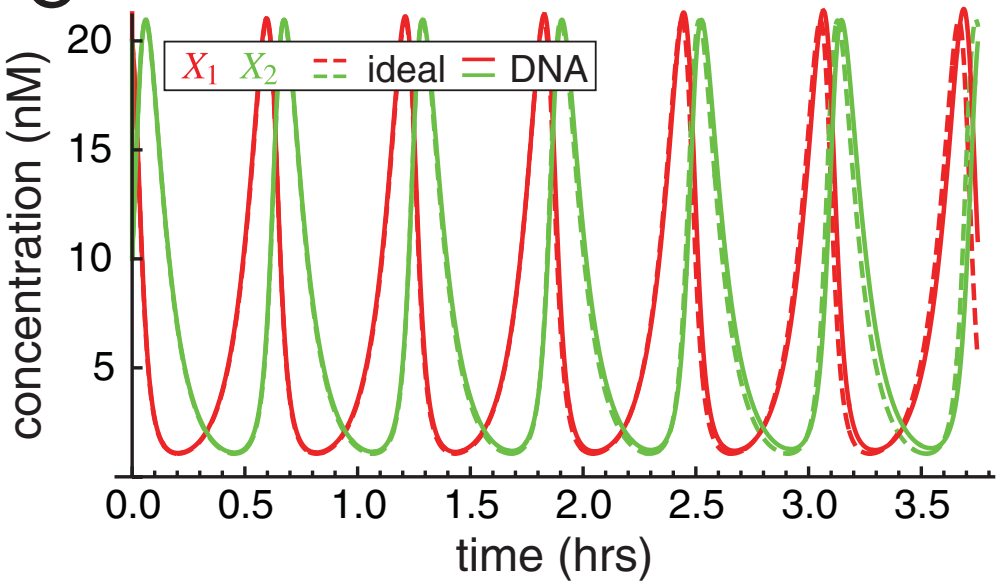

David Soloveichik, Georg Seelig, and Erik Winfree, DNA as a universal substrate for chemical kinetics, PNAS, vol. 107 no. 12, 5393–5398, www.pnas.org/cgi/doi/10.1073/pnas.0909380107

Lotka–Volterra Chemical Oscillator:

(B) Reaction modeling of DNA implementation:

- Each CRN reaction corresponds to a set of DNA reactions.
- Concentration oscillations are in the range of about 0–2.
- Under typical nucleic-acid experimental conditions, maximal second-order rate constants for strand displacement reactions are about 106/M/s, and maximum concentrations are on the order of 10–5 M.

Scaling:

- We scale the original system by a time-scaling factor of α = 300, and
- A concentration-scaling factor β = 10^{-8} employs units of seconds and molar, and
- use $C_{max} = 10^{-5}$ M and q_{max} = 106/M/s.
- Maximum strand displacement rate constant $q_{max} = 106$ $M^{-1} s^{-1}$.

Initial Concentrations:

- initial concentration of auxiliary species G_i, T_i, L_i, B_i, LS_j, and BS_j is C_{max} = 10 µM.
- The initial concentrations of strands X_1 and X_2 is γ^{-1} 20 nM = 40 nM and γ^{-1}10 nM = 20 nM.

Buffering:- Species X_2 requires a buffering module because $\sigma_2 < \sigma$ ($\sigma = \sigma_1 = k_1$ and $\sigma_2 = 0$).

- Buffering-scaling factor $\gamma^{-1} = q_{max}(q_{max} - \sigma)^{-1} = 2$.

B DNA reaction modules

$$1\left\{\begin{array}{l} X_1 + L_1 \underset{q_{max}}{\overset{q_1}{\rightleftharpoons}} H_1 + B_1 \\ X_2 + H_1 \xrightarrow{q_{max}} O_1 \\ O_1 + T_1 \xrightarrow{q_{max}} 2X_2 \end{array}\right.$$

buffering module

$$X_2 + LS_2 \underset{q_{max}}{\overset{qs_2}{\rightleftharpoons}} HS_2 + BS_2$$

$$2\left\{\begin{array}{l} X_1 + G_2 \xrightarrow{q_2} O_2 \\ O_2 + T_2 \xrightarrow{q_{max}} 2X_1 \end{array}\right.$$

$$3\left\{ X_2 + G_3 \xrightarrow{q_3} O_3 \right.$$

$$q_1 = \gamma^{-1} k_1$$

$$q_2 = \gamma^{-1} k_2 C_{max}^{-1}$$

$$q_3 = \gamma^{-1} k_3 C_{max}^{-1}$$

$$qs_2 = \gamma^{-1}(\sigma - \sigma_2)$$

C Simulation of ideal and DNA reactions

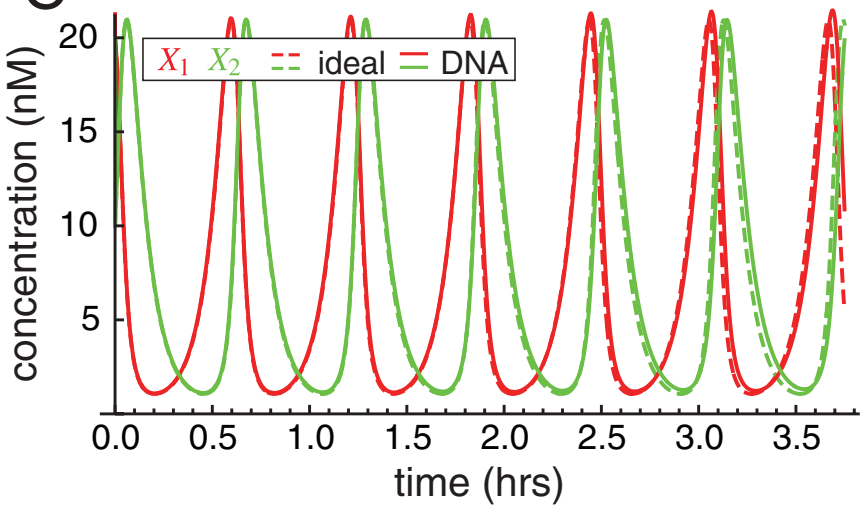

(C) Plot of the concentrations of X_1 (Red curve) and X_2 (Green curve) for the ideal system (Dashed line) and th corresponding DNA species (Solid line).

David Soloveichik, Georg Seelig, and Erik Winfree, DNA as a universal substrate for chemical kinetics, PNAS, vol. 107 no. 12, 5393–5398, www.pnas.org/cgi/doi/10.1073/pnas.0909380107

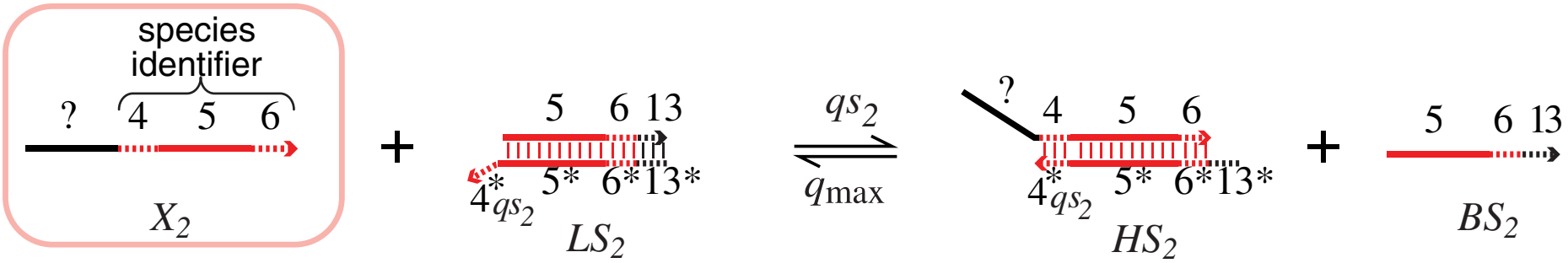

Buffering module: **DNA implementation of the buffering module used to cancel out the buffering effect.**

- **A buffering module is needed for each formal species X_j for which $\sigma_j < \sigma$.**
- **The buffering module for species X_2 is shown.**
- **X_2 reversibly displaces BS_2 from complex LS_2 to produce complex HS_2 similarly to the first reaction of the bimolecular module.**
- **The black domain (13) is unique to this buffering module for species X_2.**
- **Set $qs_j = \gamma^{-1}(\sigma - \sigma_j)$.**

$$X_j + LS_j \underset{q_{max}}{\overset{qs_j}{\rightleftharpoons}} HS_j + BS_j \quad [12] \qquad \text{simplify} \Rightarrow \qquad X_j \underset{q_{max}C_{max}}{\overset{qs_jC_{max}}{\rightleftharpoons}} HS_j \quad [13]$$

Reaction equations 12 are used in simulations;
Simplified reaction equations 13 are useful for analysis.

David Soloveichik, Georg Seelig, and Erik Winfree, DNA as a universal substrate for chemical kinetics, PNAS, vol. 107 no. 12, 5393–5398, www.pnas.org/cgi/doi/10.1073/pnas.0909380107

Programming chemical kinetics: engineering dynamic reaction networks with DNA strand displacement

PhD Thesis, Niranjan Srinivas (2015)

(Used DNA Strand Displacement Reactions to Create Oscillators)

Examples of formal CRNs exhibiting different dynamical behaviors in the mass action setting (based on numerical solutions to mass action ODEs).

(From PhD Thesis, Niranjan Srinivas)

a stabilization

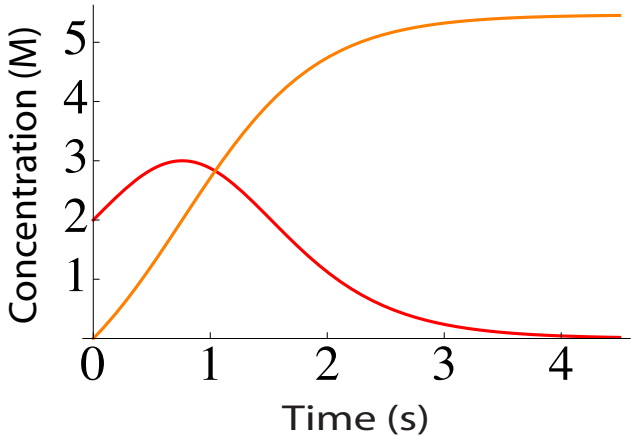

$$A \xrightarrow{1} B$$
$$A + B \xrightarrow{0.5} B$$
$$A \xrightarrow{2} 2A$$

$([A],[B])_0 = (2,0)$ M

b oscillation

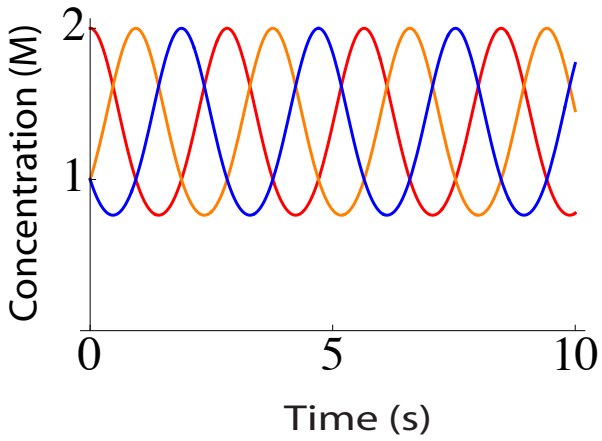

$$B + A \xrightarrow{1} 2B$$
$$C + B \xrightarrow{1} 2C$$
$$A + C \xrightarrow{1} 2A$$

$([A],[B],[C])_0 = (2,1,1)$ M

c chaos

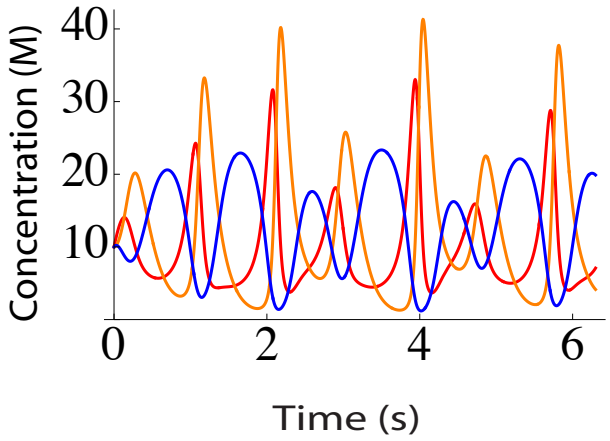

$$A \xrightarrow{30} 2A$$
$$2A \xrightarrow{0.5} A$$
$$B + A \xrightarrow{1} 2B$$
$$B \xrightarrow{10}$$
$$A + C \xrightarrow{1}$$
$$C \xrightarrow{16.5} 2C$$
$$2C \xrightarrow{0.5} C$$

$([A],[B],[C])_0 = (10,10,10)$ M

Rock-Paper-Scissors Oscillator:

- A is rock,
- B is paper, and
- C is scissors.

It has 3 autocatalytic reactions:

B+A → 2B (paper covers rock),

C+B → 2C (scissors cuts paper), and

A+C → 2A (rock breaks scissors),

The sum of the species A + B + C is conserved.

- If the rate constants for the three autocatalytic reactions are identical, the product A × B × C is also conserved.
- So the dynamics is constrained to be:
  - on the intersection of the plane A + B + C = constant and
  - the curve A × B × C = constant
- But there is no equilibrium on that intersection, resulting in characteristic triangle-like orbits.

(From PhD Thesis, Niranjan Srinivas)

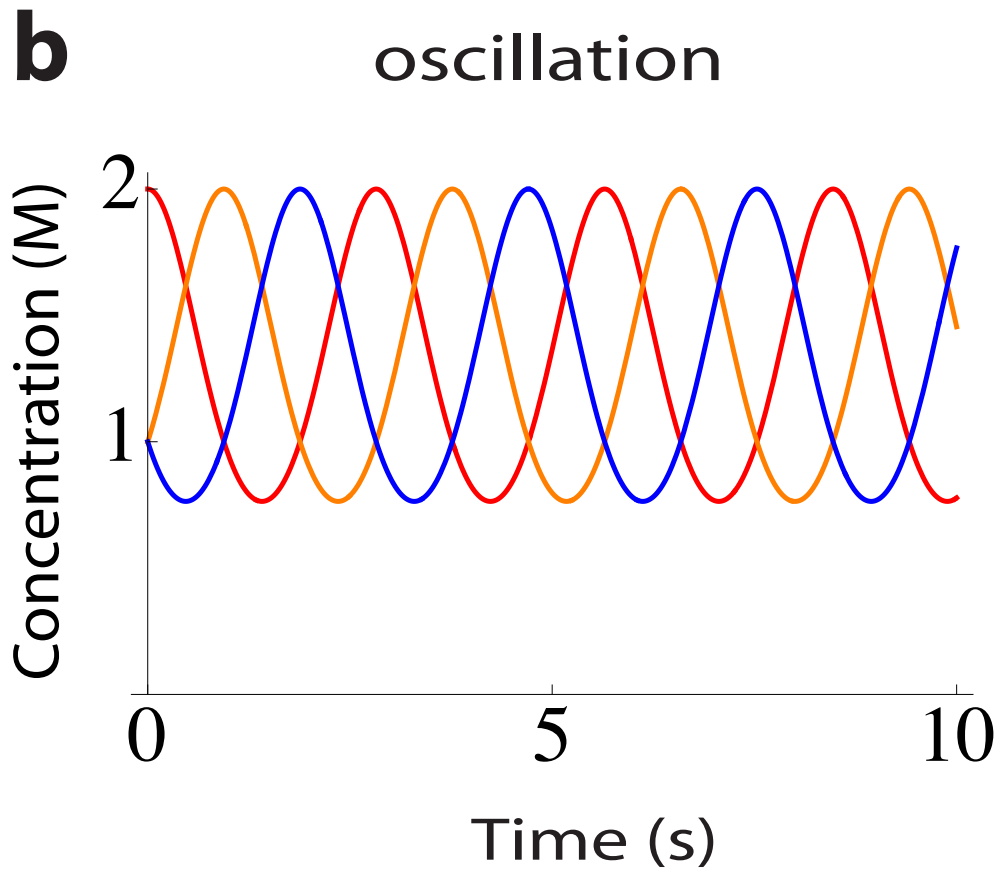

$$B + A \xrightarrow{1} 2B$$

$$C + B \xrightarrow{1} 2C$$

$$A + C \xrightarrow{1} 2A$$

$$([A], [B], [C])_0 = (2, 1, 1)\ M$$

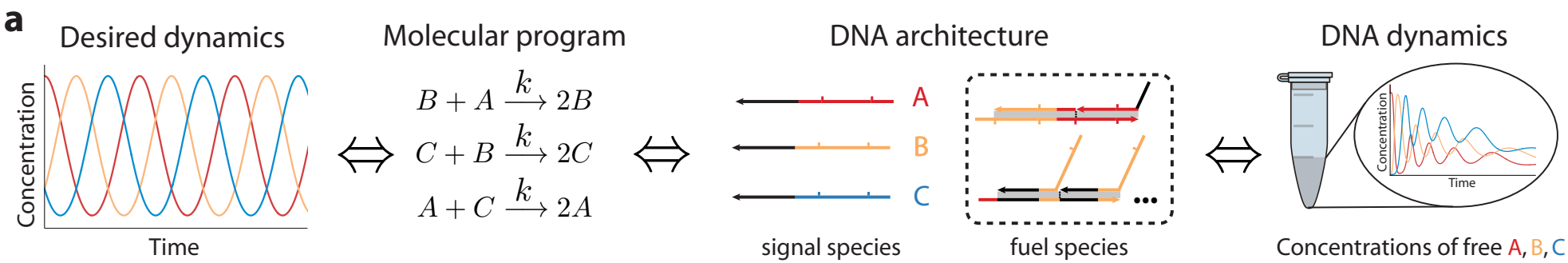

Overview of CRN-to-DNA implementation:

- Start with a desired dynamical behavior (oscillation, in this case) and a CRN program that captures the desired dynamics.
- We then use the CRN-to-DNA scheme described in this chapter to translate the formal CRN into a DNA strand displacement implementation, where the formal species are represented by single strands of DNA called "signal" species.

- Desired reactions between signal species are mediated by "fuel" species which provide both logic and free-energy for the reaction.
- Some of the fuel species are multistranded complexes which are pre-prepared and purified. In the regime where the fuel species are at high concentration, the signal species approximate the dynamics of the formal species in the original CRN.

- Reactions are performed in "batch reactor" mode, which means that fuel species are not replenished.
(Therefore, the test tube dynamics is expected to deviate from idealized formal CRN dynamics.)
(From PhD Thesis, Niranjan Srinivas)

Domain notation: A "domain" comprises contiguously located bases whose binding and unbinding occurs as one logical unit.
* indicates Watson-Crick complementarity.
Arrows indicate 3' ends.

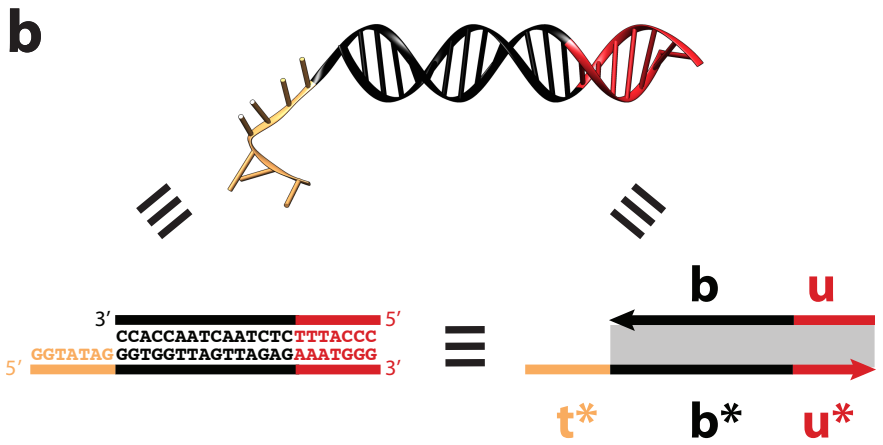

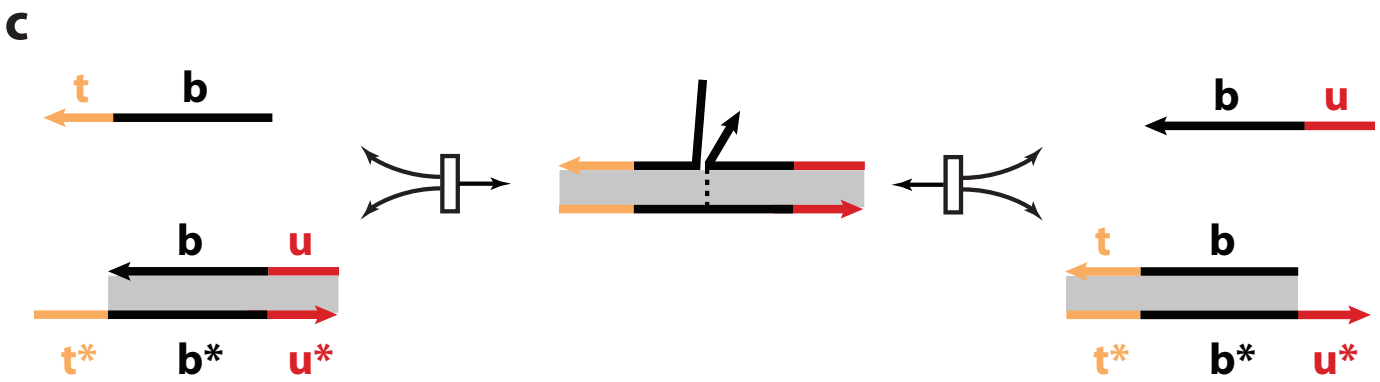

Toehold exchange Reaction: "Short" (5-7 nucleotide) domains which bind fleetingly to their components at room temperature and reversibly co-localize distinct molecules are called "toeholds".

- Here toehold t reversibly co-localizes the molecules to form a three stranded intermediate, where the two b domains can exchange base pairs by a process called three-way branch migration.
- Eventually, either toehold u dissociates (leading to the products) or toehold t dissociates (leading to the reactants).
- Notice that the entire process is reversible and toehold u can also carry out toehold exchange.

(From PhD Thesis, Niranjan Srinivas)

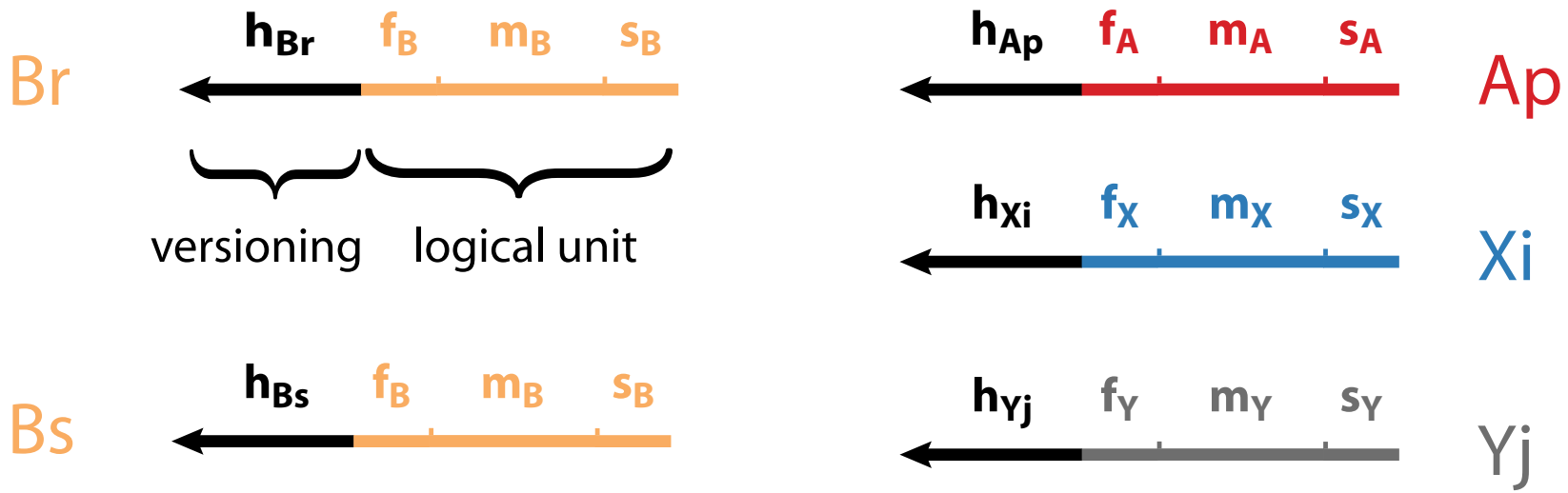

The formal species are represented by single-stranded DNA molecules (signal strands):

- With a history domain in black (versioning unit, e.g. h_{Br}) and a logical unit.
- The logical unit with three domains:
  - the first toehold (e.g. f_B),
  - a branch migration region (e.g. m_B), and
  - the second toehold (e.g. s_B).
- Signal strands are designed to not interact with each other.

- Signal strands with the same logical unit (e.g. B_r and B_s) represent the same formal species (B) and are designed to behave identically in solution.

(From PhD Thesis, Niranjan Srinivas)

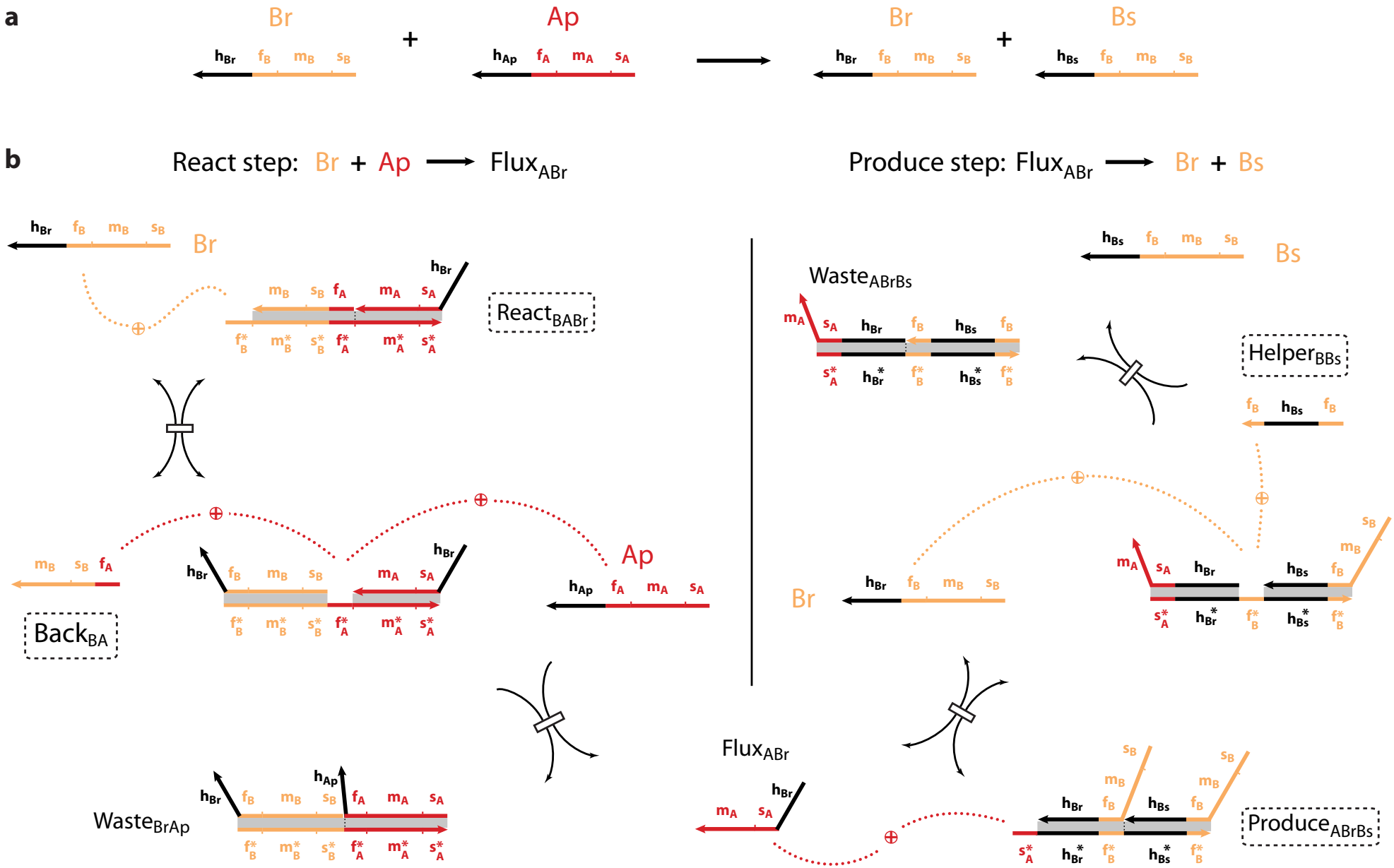

DNA Strand-Displacement Implementation of Cyclic Rock-Paper-Scissors Oscillator Module 1: Reaction B + A → 2B.

- **The same mechanism can occur with *different versions of B and A.***
- ***Names of fuel species are enclosed in a dashed box.***

(From PhD Thesis, Niranjan Srinivas)

Kinetic Model for Simulation of DNA Strand-Displacement Implementation of Cyclic Lotka-Volterra Oscillator

Module 1: Reaction B + A → 2B:

$$\mathrm{B} + \mathrm{React}_{\mathrm{BABr}} \underset{k_{\mathrm{sd}}}{\overset{k_{\mathrm{sd}}}{\longleftrightarrow}} \mathrm{ReactInt}_{\mathrm{BABr}} + \mathrm{Back}_{\mathrm{BA}}$$

$$\mathrm{ReactInt}_{\mathrm{BABr}} + \mathrm{A} \xrightarrow{k_{\mathrm{sd}}} \mathrm{Flux}_{\mathrm{ABr}} + \mathrm{Waste}_{\mathrm{BA}}$$

$$\mathrm{Flux}_{\mathrm{ABr}} + \mathrm{Produce}_{\mathrm{ABrBs}} \underset{k_{\mathrm{sd}}}{\overset{k_{\mathrm{sd}}}{\longleftrightarrow}} \mathrm{B} + \mathrm{ProduceInt}_{\mathrm{ABrBs}}$$

$$\mathrm{ProduceInt}_{\mathrm{ABrBs}} + \mathrm{Helper}_{\mathrm{BBs}} \xrightarrow{k_{\mathrm{sd}}} \mathrm{B} + \mathrm{Waste}_{\mathrm{ABrBs}}$$

- Equations above specify the chemical reaction equations in the strand-displacement level model for the autocatalytic module B + A → 2B.

- Each strand displacement and toehold exchange reaction has been modeled as an effective bimolecular reaction with a *rate constant* of k_{sd} = 2 × 10^5 /M /s.

- This model assumes that *unimolecular reactions* (including dissociation of toeholds and branch migration) are *effectively instantaneous*.

- All fuel molecules have an initial concentration of 300 nM and are *not replenished*.

(From PhD Thesis, Niranjan Srinivas)

DNA Strand-Displacement Implementation of Cyclic Lotka-Volterra Oscillator

Module 2: Reaction C + B → 2C.

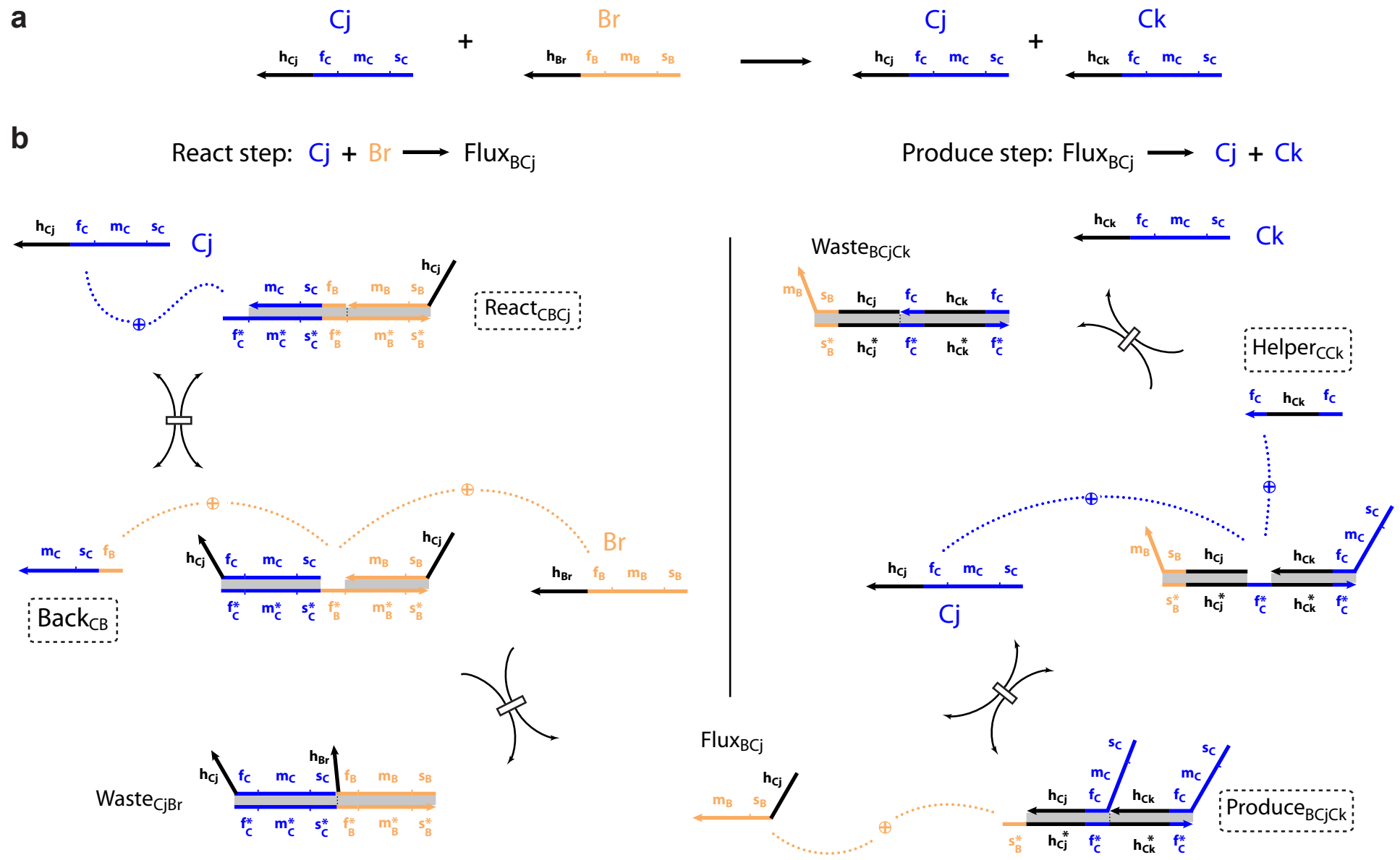

The same mechanism can occur with different versions of C and B.

Names of fuel species are enclosed in a dashed box. ***(From PhD Thesis, Niranjan Srinivas)***

DNA Strand-Displacement Implementation of Cyclic Lotka-Volterra Oscillator

Module 3: Reaction A + C → 2A.

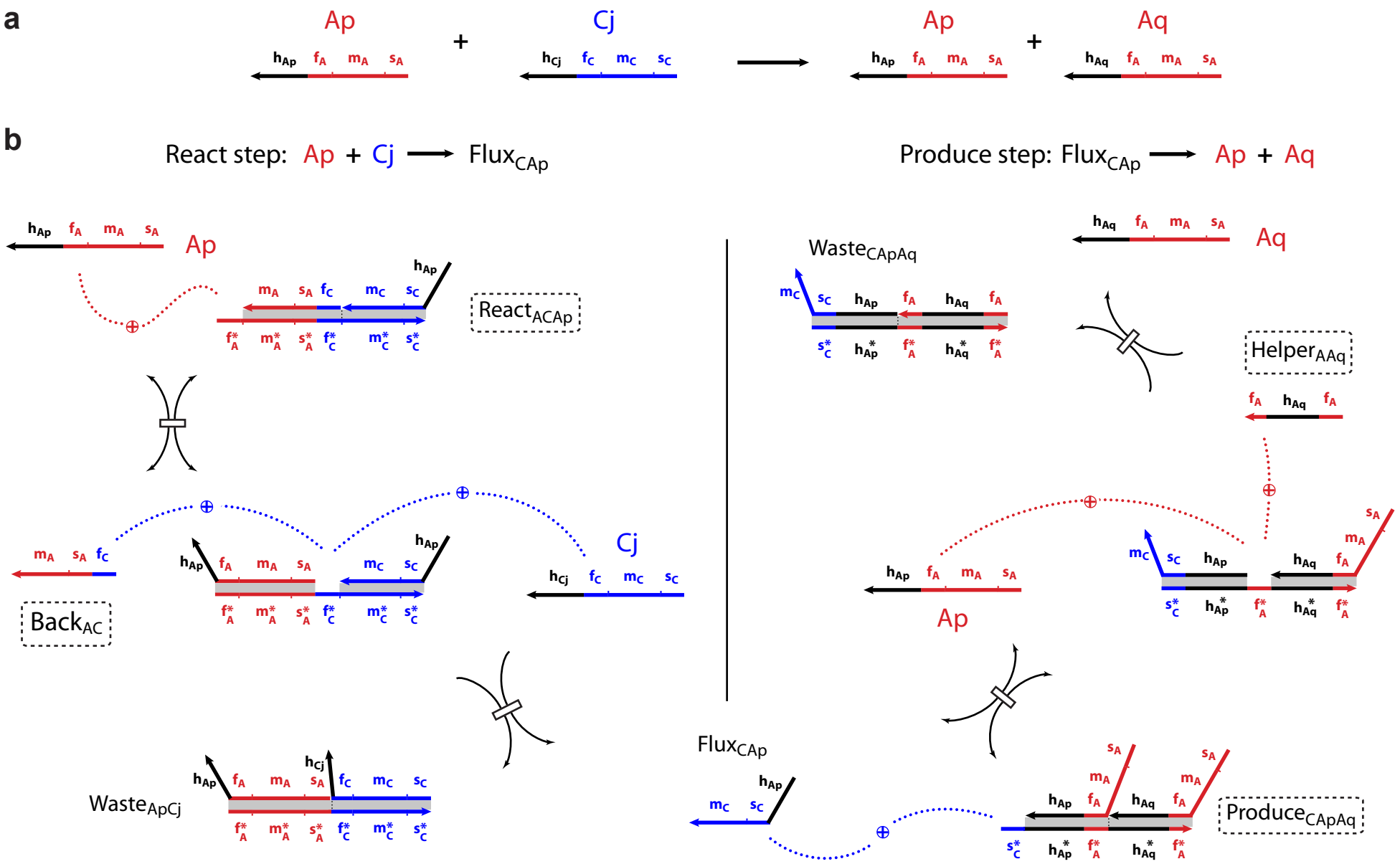

The same mechanism can occur with different versions of A and C. Names of fuel species are enclosed in a dashed box. ***(From PhD Thesis, Niranjan Srinivas)***

Modeling of DNA Strand-Displacement Implementation of Cyclic Rock-Paper-Scissors Oscillator: **Modeling the DNA implementation of the oscillator at the level of individual strand displacement and toehold exchange reactions.**

The fuel species are present at an initial concentration of 300 nM and are not replenished

a $([A],[B],[C])_0 = (30, 10, 10)$ nM

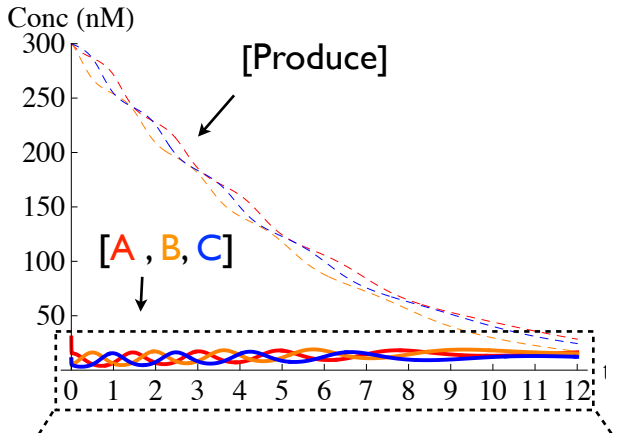

a. Concentrations of Product molecules (dashed lines; - -- ProduceCApAq in red, ProduceBCjCk in blue, ProduceABrBs in orange) and signal strands as a function of time starting with an initial concentration of ([A], [B], [C])0 = (30, 10, 10) nM.

b

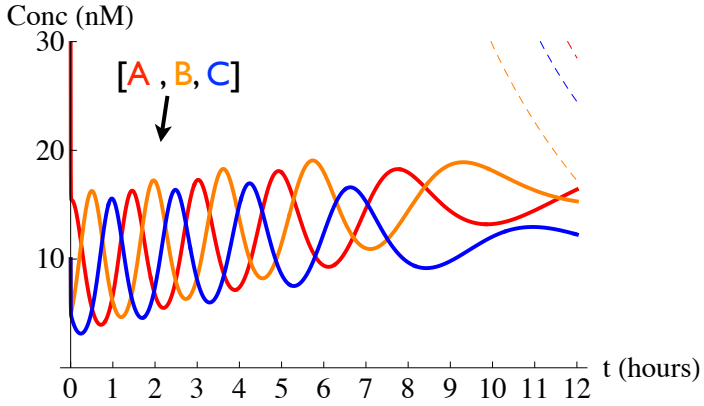

b. The plot in (a), zoomed in so that the oscillatory dynamics of the signal strands are visible

$([A],[B],[C])_0 = (60, 10, 10)$ nM

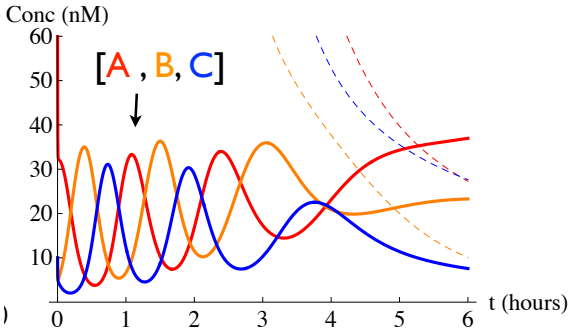

c. The plot in (b) with an initial concentration of ([A], [B], [C]) = (60, 10, 10) nM, all other parameters being the same.

(From PhD Thesis, Niranjan Srinivas)

Leak Pathways:

Examples of spurious "leak" pathways that arise due to blunt-end (zero base toehold) strand displacement.

- These pathways are illustrated in the case of the autocatalytic module C + B → 2C but can occur with the other modules as well.
- Locations of invasion are indicated by numbered dashed arrows.

a. The second input (here, B_r) can invade at locations 1 (the junction) and 2 (the end of the helix) in the React species. Once strand displacement finishes, the Flux molecule may be released and a spurious species can be formed.

b. A similar reaction can happen between the Helper species and the Produce species, releasing the second output of the Produce molecule (here, C_k) and resulting in a spurious species.

c. Spontaneous fraying due to thermal fluctuations at the end of the helix in the React molecule may enable the Produce molecule to invade at at location 5. Strand displacement can then result in the release of the first output of the produce gate (here, C_j) and the formation of a spurious species. Notice that all of these spurious species shown here are capable of participating in some reactions that are also a legitimate part of desired reaction pathways.

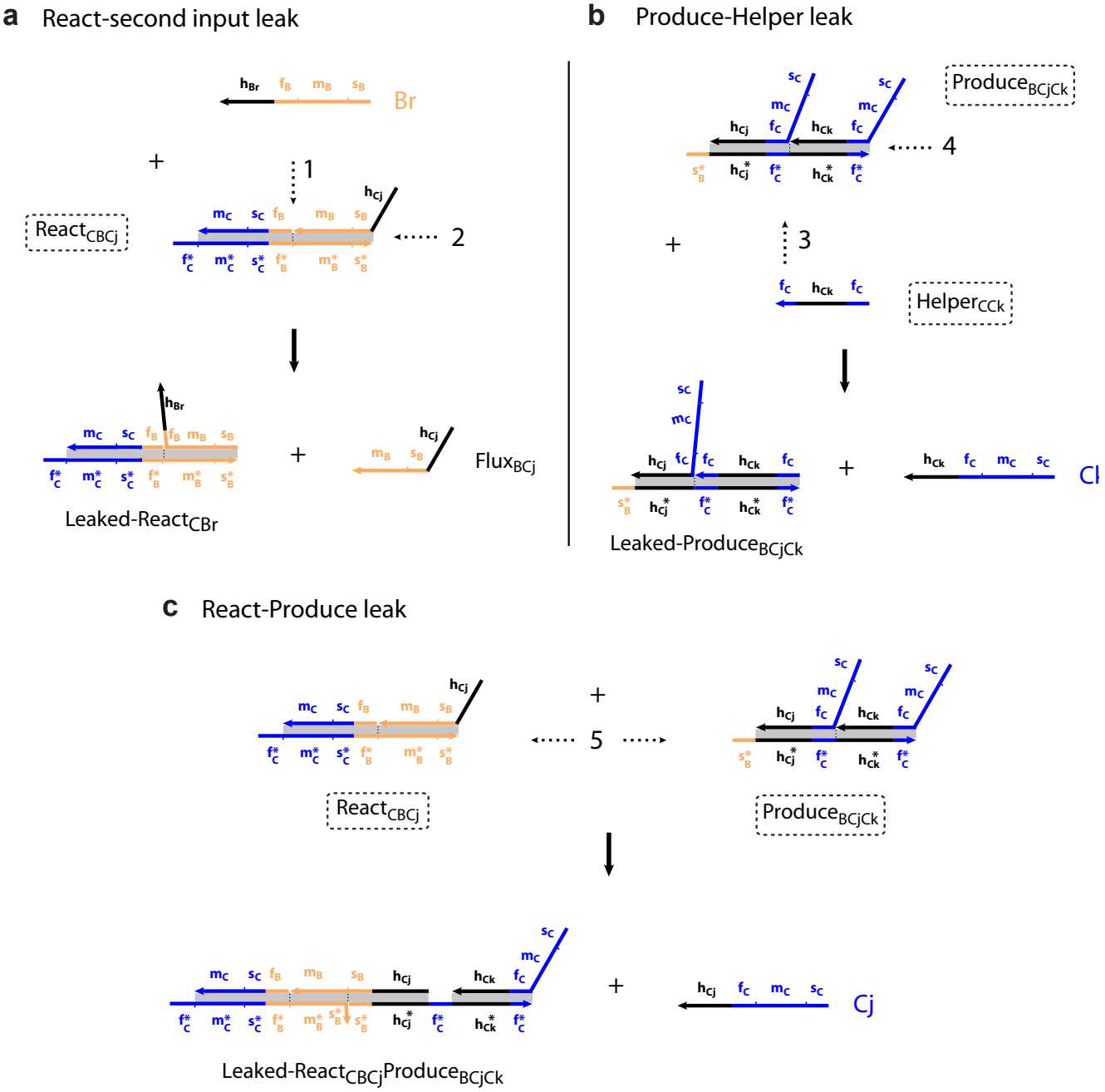

(From PhD Thesis, Niranjan Srinivas)

Programming an in vitro DNA oscillator using a molecular networking strategy

Kevin Montagne, Raphael Plasson, Yasuyuki Sakai, Teruo Fujii and Yannick Rondelez

Molecular Systems Biology 7; Article number 466, 2010
doi:10.1038/msb.2010.120

(Used DNA Polymerase and Nickase Enzymic Reactions to Create Oscillators)

(A) Schematic description of the canonical gene regulation pathway.

‘--->‘ Indicates an activation interaction

‘---|’ Indicates inhibition

‘---o’ represents either activation or inhibition

‘-+’ indicates decay.

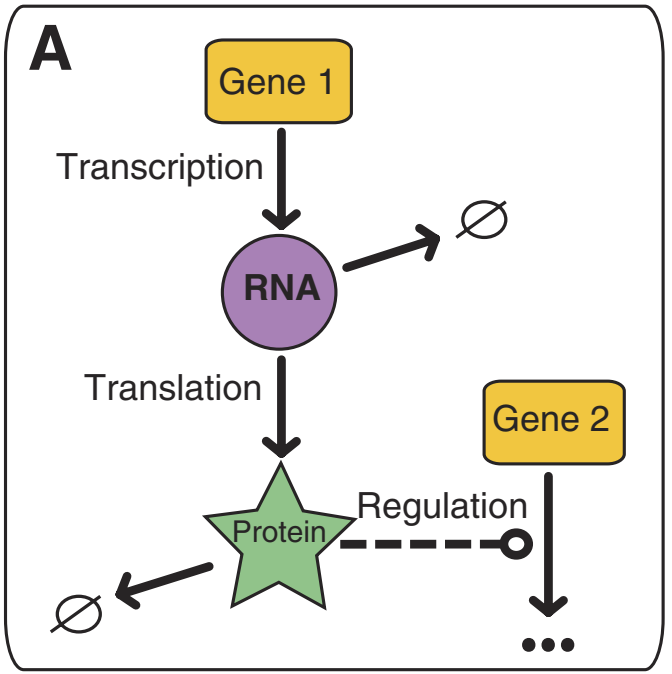

(B) A similar architecture is implemented, but genes are replaced by single-stranded DNA templates, while dynamic species (RNA and proteins) are replaced by small oligomers obtained from replication of the templates.

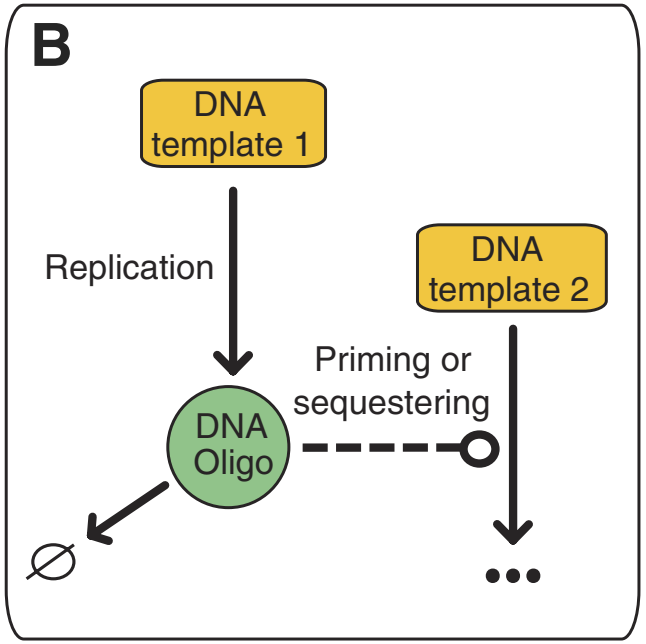

Kevin Montagne, Raphael Plasson, Yasuyuki Sakai, Teruo Fujii and Yannick Rondelez, Programming an in vitro DNA oscillator using a molecular networking strategy, Molecular Systems Biology 7; Article number 466; doi:10.1038/msb.2010.120

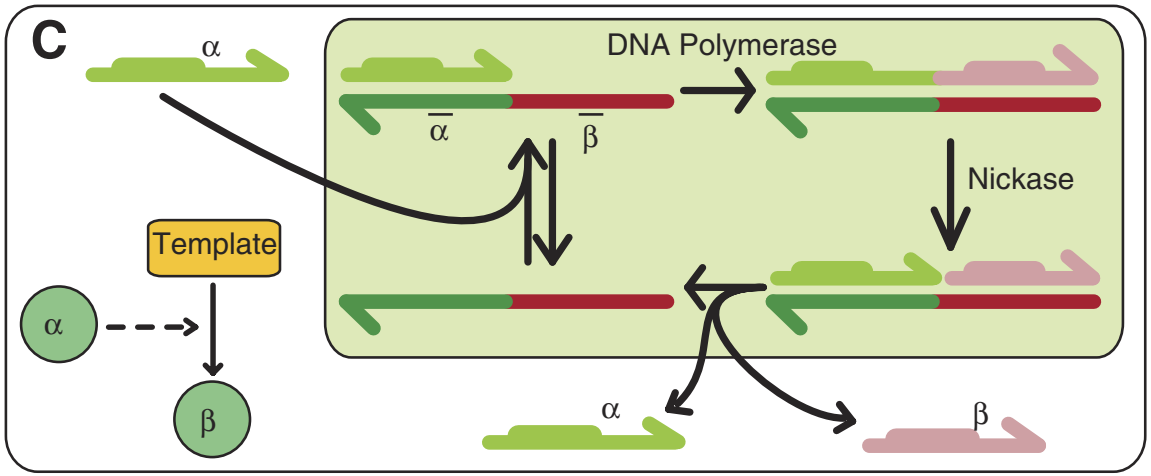

(C) Molecular description of the activation mechanism. **The input oligomer a binds to the template and is elongated by a polymerase. a displays a recognition sequence (in bold), which allows a nicking endonuclease to nick the newly extended strand. This step releases the input a, the output strand b and the template, ready for a new turnover.**

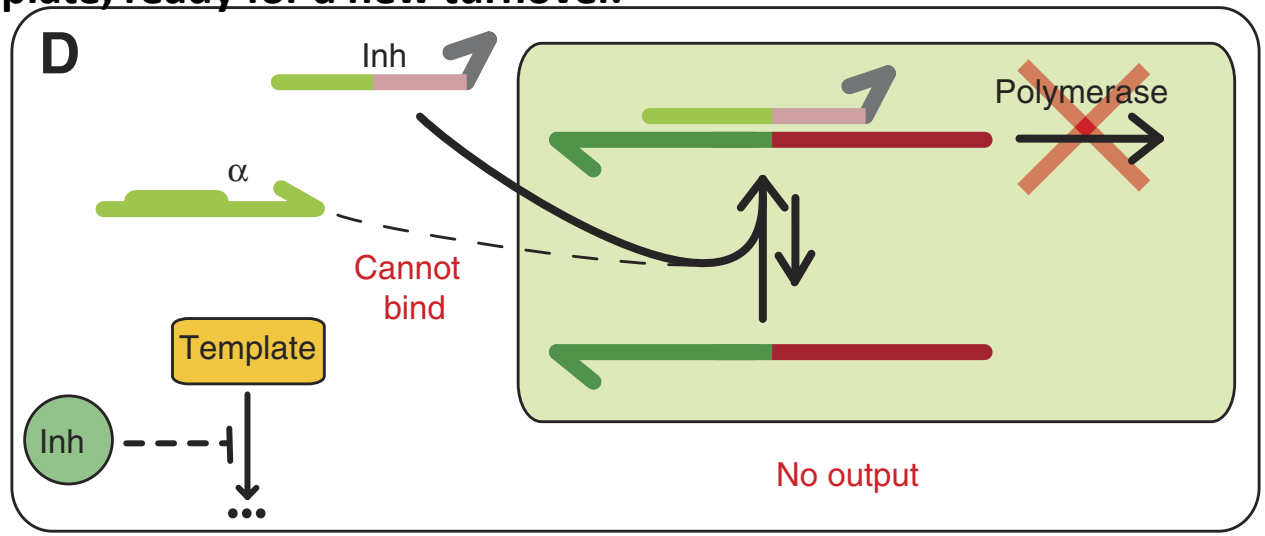

(D) Inhibition mechanism. **The inhibitor Inh is designed to bind strongly to the template but, due to a pair of mismatches at its 30 end, it is not recognized as a polymerization primer. Therefore, the template is reversibly sequestered as an unproductive partial duplex.**

Kevin Montagne, Raphael Plasson, Yasuyuki Sakai, Teruo Fujii and Yannick Rondelez, Programming an in vitro DNA oscillator using a molecular networking strategy, Molecular Systems Biology 7; Article number 466; doi:10.1038/msb.2010.120

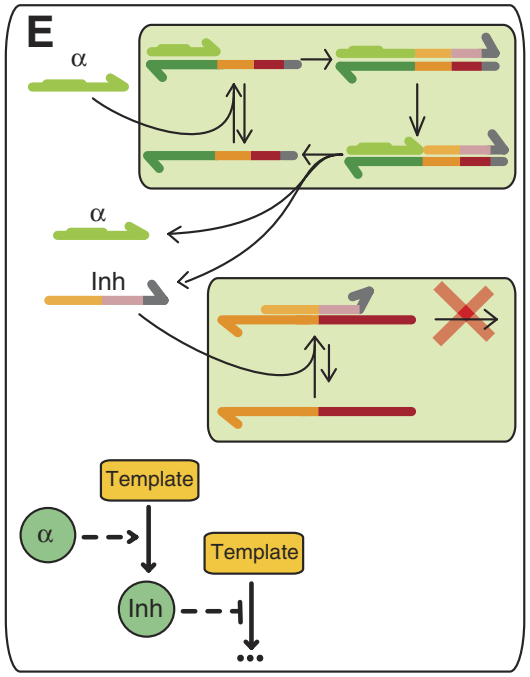

(E) Cascading: Previous activation or inhibition blocks can be connected to each other by simply matching their sequences (shown here using a color code).

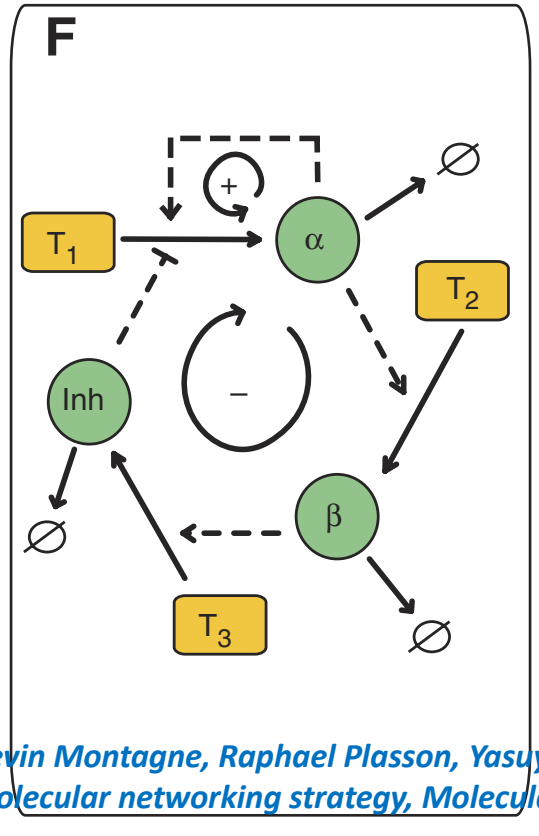

(F) Implementation: an oscillator comprising a positive-feedback loop (+) and a delayed negative- feedback loop (-).

Kevin Montagne, Raphael Plasson, Yasuyuki Sakai, Teruo Fujii and Yannick Rondelez, Programming an in vitro DNA oscillator using a molecular networking strategy, Molecular Systems Biology 7; Article number 466; doi:10.1038/msb.2010.120

Experiments: Reactions shown were performed at 38.51C, initiated with 0.1 nM a and monitored (ex. 490 nM; em. 510 nM) using EvaGreen- induced fluorescence.

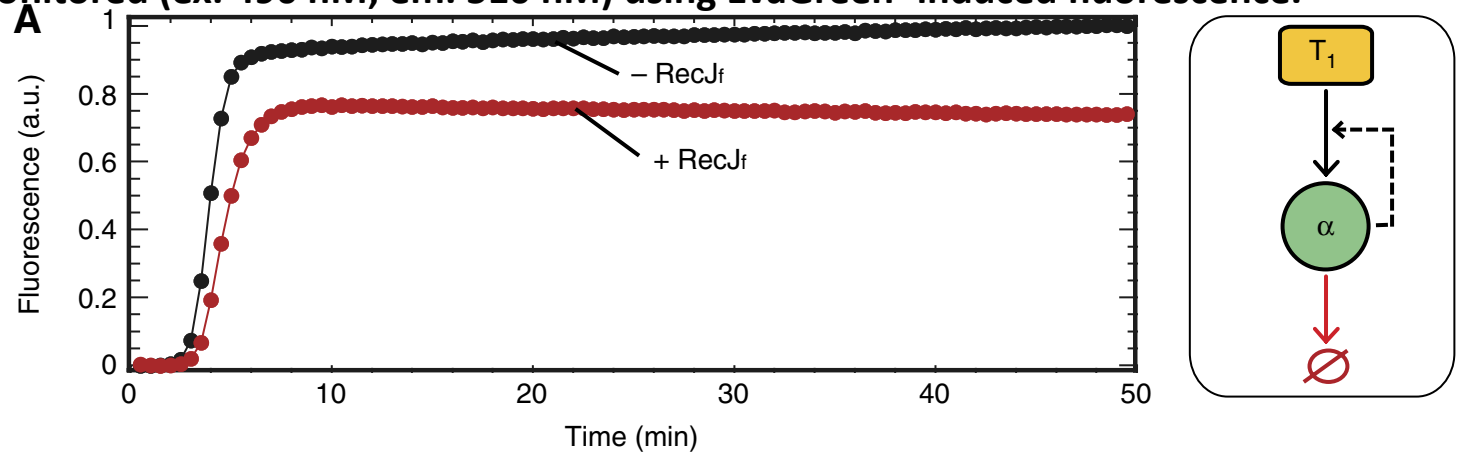

(A) One-node positive-feedback loop (autocatalytic module):

- In the presence of *Bst Polymerase* (80 U ml 1) and *nicking enzyme Nt.bstNBI* (200 U ml 1), template T_1 (60 nM) performs an - exponential amplification of its input a.
- The fluorescence reaches a plateau when the template gets saturated with a.
- The low subsequent increase is due to the accumulation of single-stranded a, weakly fluorescent in these conditions.
- In the presence of *exonuclease RecJ*$_f$ (30 U ml 1), the reaction reaches a flat steady state instead.

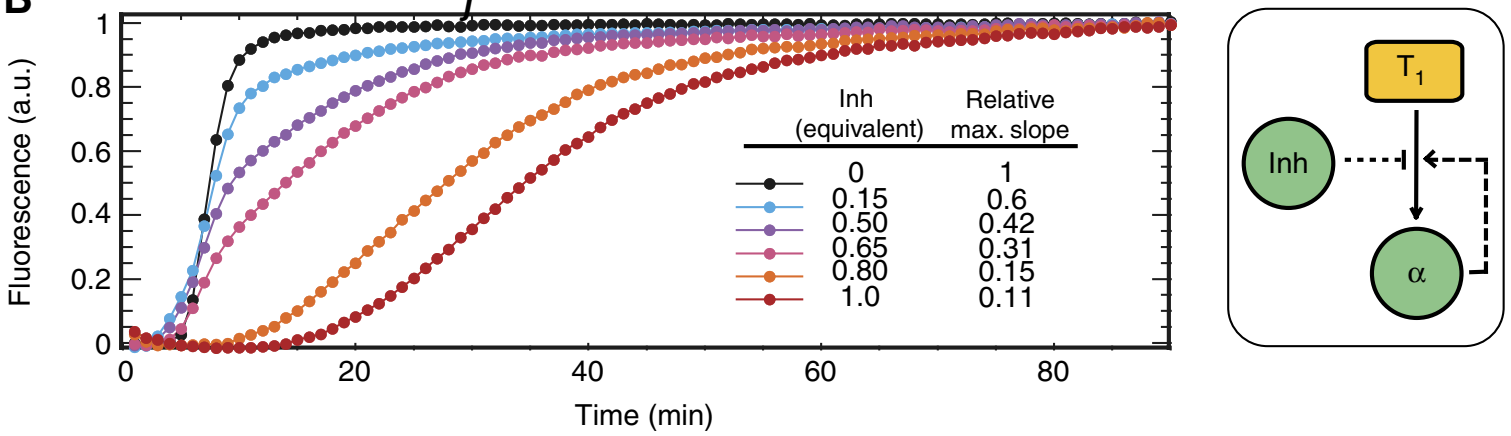

(B) Inhibited amplification: Increasing amounts of inhibitor (from 0 to 1 eq. of T_1) decreases the amplification rate of the previous system (RecJ$_f$).

Kevin Montagne, Raphael Plasson, Yasuyuki Sakai, Teruo Fujii and Yannick Rondelez, Programming an in vitro DNA oscillator using a molecular networking strategy, Molecular Systems Biology 7; Article number 466; doi:10.1038/msb.2010.120

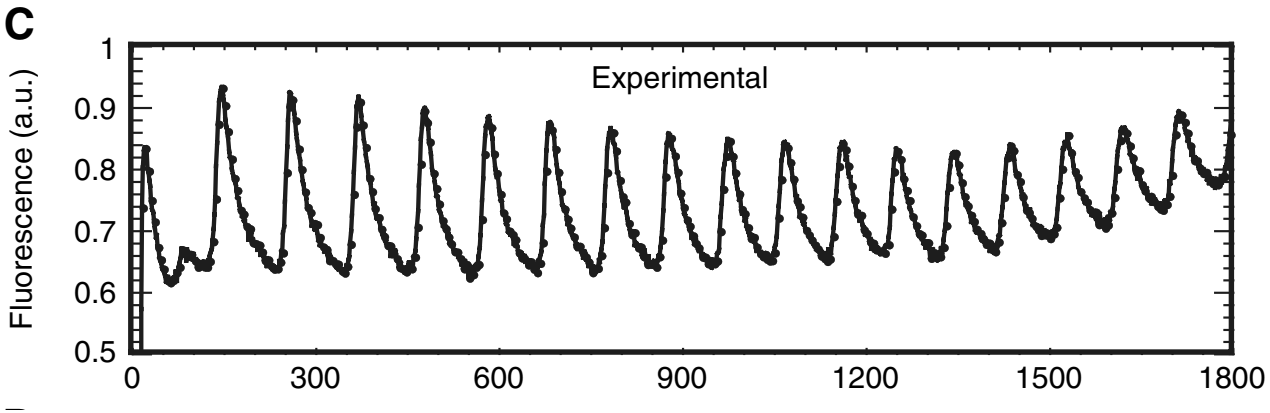

(C) Oscillator.

- Production of Inh is connected to the presence of a as in Figure 1F.
- This three-templates (T_1 and T_3 : 30 nM; T_2 : 5 nM) three- enzymes (Bst, Nt.BstNBI, RecJ$_f$) system produces sustained fluorescent oscillations with a period of 100 min.
- Agrees with predicted evolution of total concentration of base pairs (D).

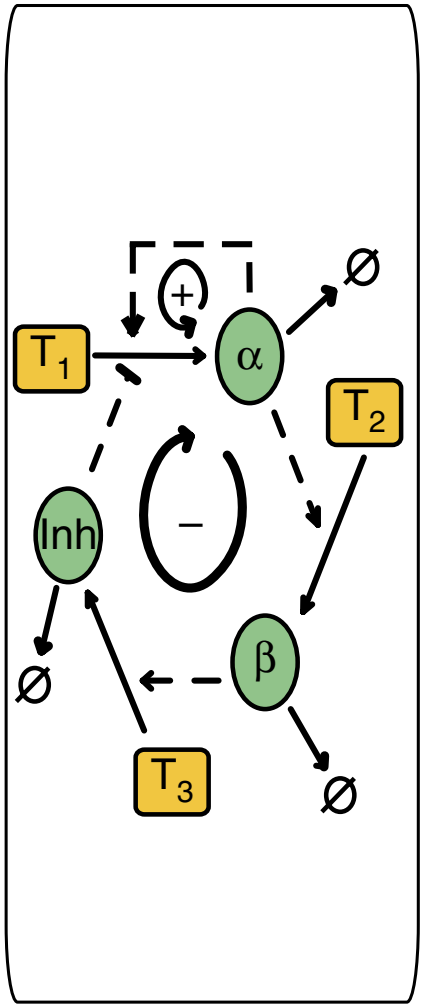

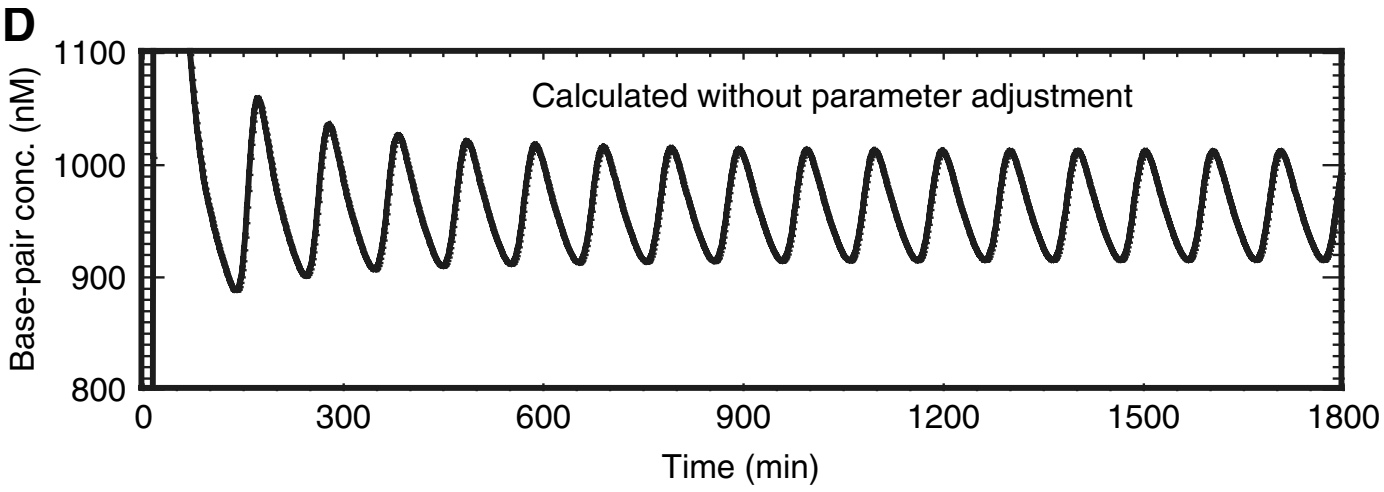

Kevin Montagne, Raphael Plasson, Yasuyuki Sakai, Teruo Fujii and Yannick Rondelez, Programming an in vitro DNA oscillator using a molecular networking strategy, Molecular Systems Biology 7; Article number 466; doi:10.1038/msb.2010.120

Synthetic in vitro transcriptional oscillators

Jongmin Kim and Erik Winfree

Molecular Systems Biology 7, Article number 465, 2010
doi:10.1038/msb.2010.119

Supplementary Info:
http://www.dna.caltech.edu/Papers/transcriptional_oscillators2011_SI.pdf

(Used DNA Hybridization and Enzyme Reactions to Create Oscillators)

Schematics for vitro transcriptional oscillators.

(A) Reaction diagram for the two-switch negative-feedback oscillator.

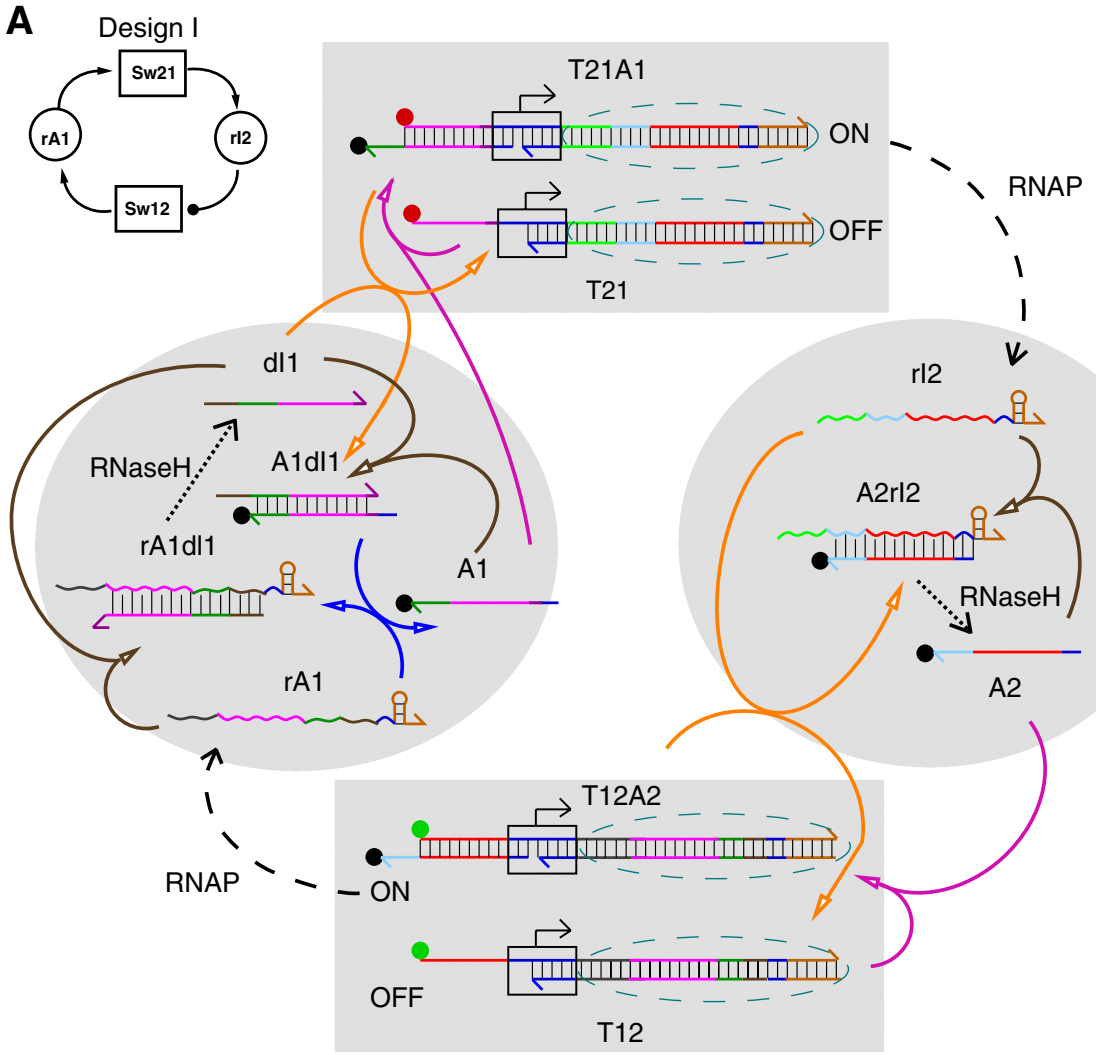

- On the top left is a block diagram, wherein arrowheads indicate activation or production and circular ends indicate inhibition.
- The block diagram corresponds to the detailed diagram as highlighted by gray shading:
- T21A1 (ON-state switch Sw21) and T21 (OFF-state switch Sw21) are summarized by the Sw21 block;
- RNA inhibitor rI2, together with its threshold, DNA activator A2, and their complex, A2rI2, is summarized by the rI2 block; and
- similarly for the Sw12 and rA1 blocks.

Coloring:- The sequence domains are color coded to indicate identical or complementary sequences; for the switch templates, the dark blue sequence domain inside the rectangle indicates the T7 RNAP promoter sequence with arrows pointing in the direction of transcription, with transcription domains indicated by light blue dashed circles.

- Transcription by RNAP is shown as black dashed arrows - Degradation of RNA within RNA-DNA hybrids by RNase H is shown as black dotted arrows.
- Hybridization reactions are reversible; the arrowhead corresponds to the thermodynamically favorable direction, and the reverse reactions are expected to be so slow as to be negligible

For fluorescence monitoring:

- OFF-state switches are labeled with fluorophores, T21 with Texas Red (red circle) and T12 with TAMRA (green circle), and both activators A1 and A2 are labeled with Iowa Black RQ quenchers (black circle).
- Four types of hybridization reactions are indicated by arrows: activation (magenta), inhibition (orange), annihilation (brown), and release (blue).

Jongmin Kim and Erik Winfree, Synthetic in vitro transcriptional oscillators, Molecular Systems Biology 7; Article number 465;

(B) List of hybridization and enzyme reactions.

B

Activation		T21 + A1 → T21A1		T12 + A2 → T12A2	
Inhibition		T21A1 + dI1 → T21 + A1dI1		T12A2 + rI2 → T12 + A2rI2	
Annihilation		A1 + dI1 → A1dI1		A2 + rI2 → A2rI2	
		rA1 + dI1 → rA1dI1			
Release		A1dI1 + rA1 → rA1dI1 + A1			
RNAP	(fast)	T21A1 → T21A1 + rI2	(fast)	T12A2 → T12A2 + rA1	
	(slow)	T21 → T21 + rI2	(slow)	T12 → T12 + rA1	
RNaseH		rA1dI1 → dI1		A2rI2 → A2	

(C) Theoretical end states of hybridization reactions in the absence of enzymes.

- As the input RNA inhibitor rI2 concentration increases, initially the free DNA activator A2 is consumed without affecting switch state.

- When all free A2 is consumed (i.e., $[rI2]1/4[A2^{tot}]-[T12^{tot}]$), rI2 displaces A2 from the T12A2 complex in stoichiometric amounts until all A2 is consumed (i.e., $[rI2]1/4[A2^{tot}]$), resulting in a piecewise linear graph.

- Similarly, the response of switch Sw21 to rA1 input is a piecewise linear graph.

C

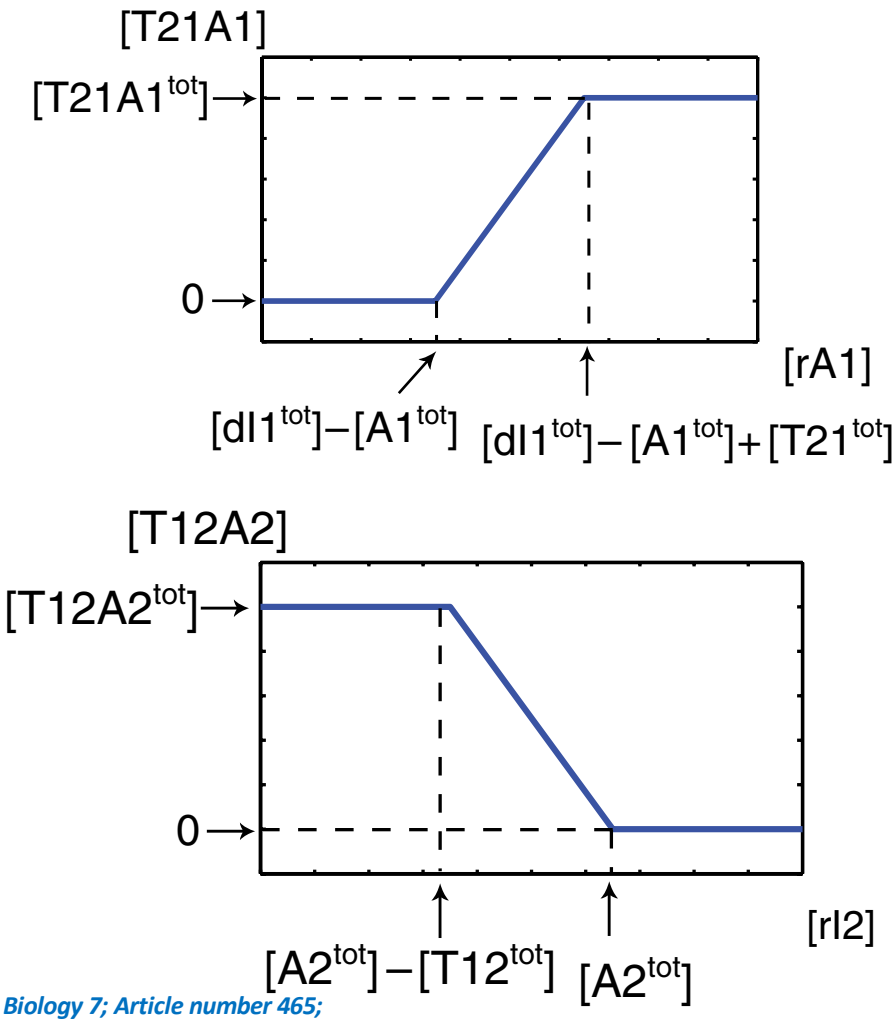

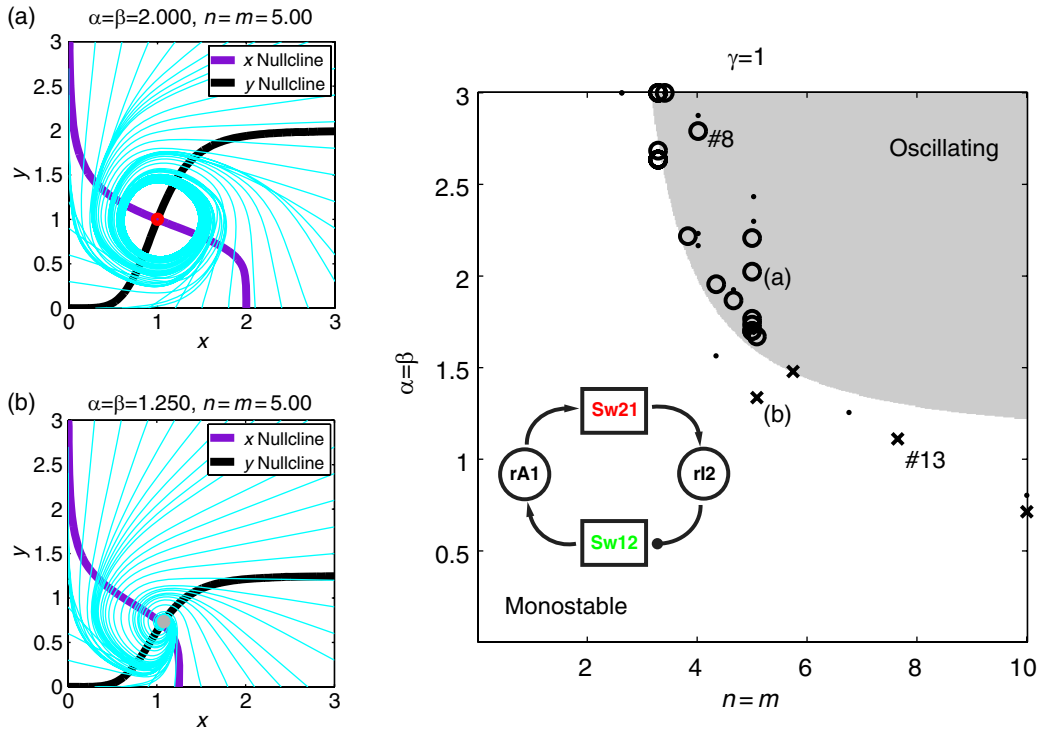

Simple model characterization and experimental results of the two-switch negative-feedback oscillator (Design I).

- The phase diagram of dynamic behaviors shows two domains with respect to changes in a and b (unitless parameters proportional to [T12^{tot}] and [T21^{tot}]) versus n and m (apparent Hill exponents of the activation and inhibition functions).

- (a, b) Phase portraits using unitless dynamic variables proportional to [rA1] and [rI2], x and y. The nullclines for x (violet lines) and y (black lines) are superimposed with temporal trajectories (cyan lines). There are fixed points where x and y nullclines intersect; stable (gray circle) and unstable (red circle) fixed points are marked.

- The system exhibits (a) limit cycle oscillation or (b) damped oscillation to a monostable steady state.

- Parameters are [T12^{tot}]1⁄4[T21^{tot}]1⁄4[A1^{tot}]1⁄4 100 nM, KA1⁄4KI1⁄41 mM, n1⁄4m1⁄45, t1⁄4500 s, g1⁄41, kd1⁄40.002/s, and respectively kp1⁄40.04/s or kp1⁄40.025/s.

- In experiments, normalized fluorescence time courses measured the percent OFF-state switch Sw12 (TAMRA-labeled T12, green) and the percent OFF-state switch Sw21 (Texas Red-labeled T21, red).

Jongmin Kim and Erik Winfree, Synthetic in vitro transcriptional oscillators, Molecular Systems Biology 7; Article number 465;

Two examples are shown:

- Reaction #8 with stable oscillations and
- Reaction #13 with strongly damped oscillations.

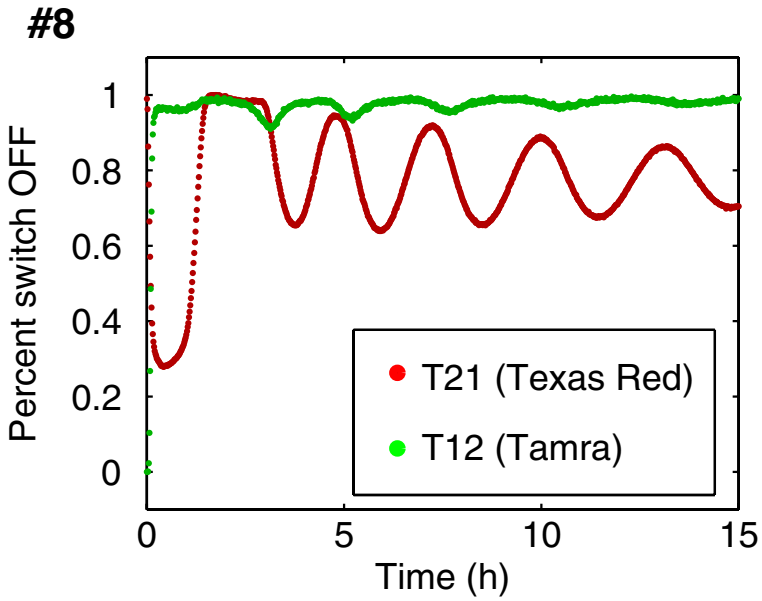

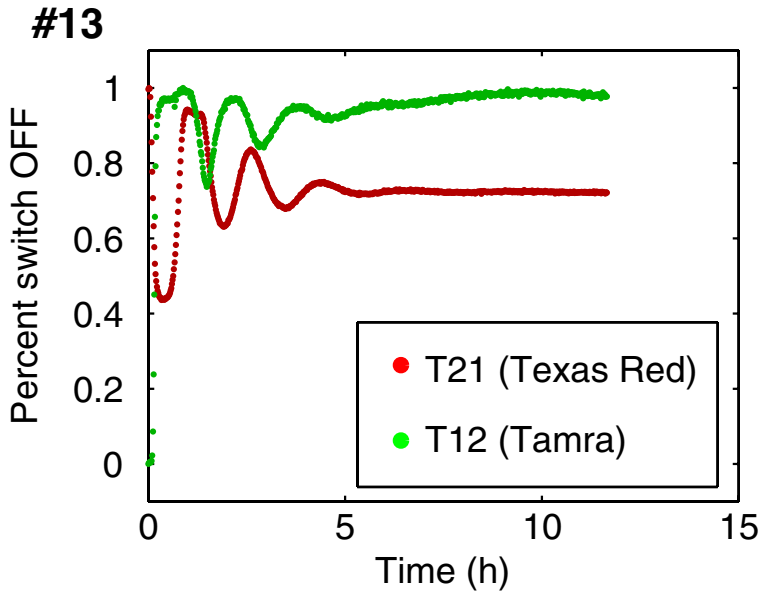

-Experimental parameters were, respectively, ([$T21^{tot}$], [$A1^{tot}$], [$dI1^{tot}$], [$T12^{tot}$], [$A2^{tot}$], [$RNAP^{tot}$], [$RNaseH^{tot}$])1⁄4(250, 250, 700, 120, 350, 92, 8.3) nM and (250, 250, 1000, 80, 500, 125, 15.0) nM.

- Reaction #13 used higher [$dI1^{tot}$], higher [$A2^{tot}$], and lower [$T12^{tot}$], compared with reaction #8.

- **Thus, reaction #13 is mapped to a higher n and a lower a than reaction #8, and lay within the monostable domain rather than the oscillating domain.**

- Experimental results were mapped to the phase diagram with respect to a reference oscillation, and shown as 'stable' (circles, damping coefficient o0.15/h), 'damped' (dots, damping coefficient between 0.15/h and 0.5/h), and 'strongly damped or too slow to measure' (crosses, damping coefficient 40.5/h) oscillations.

Jongmin Kim and Erik Winfree, Synthetic in vitro transcriptional oscillators, Molecular Systems Biology 7; Article number 465;

Experimental characterization of a two-switch negative feedback oscillator.

(A) The fluorescence time courses report the OFF-state switch Sw12 (TAMRA-labeled T12, green) and the OFF-state switch Sw21 (Texas Red-labeled T21, red); corresponding extended model fits are shown as lines in lighter shades. The non-denaturing gel measurement of the OFF-state Sw21 (black squares, from C below) showed reasonable agreement with fluorescence results.

(B) The total rI2 concentration measurement (blue circles, from C below) showed five complete oscillation cycles; extended model fits are shown as lines (light blue). The concentration of incomplete degradation products was estimated from the band of E35 nucleotides in the denaturing gel (magenta). The rA1 concentration was not measured because most bands were not significantly above background.

(C) The concentrations of RNA signals and incomplete degradation products were measured in a denaturing gel (top and middle) and the OFF-state switch concentrations were measured in a non- denaturing gel (bottom)

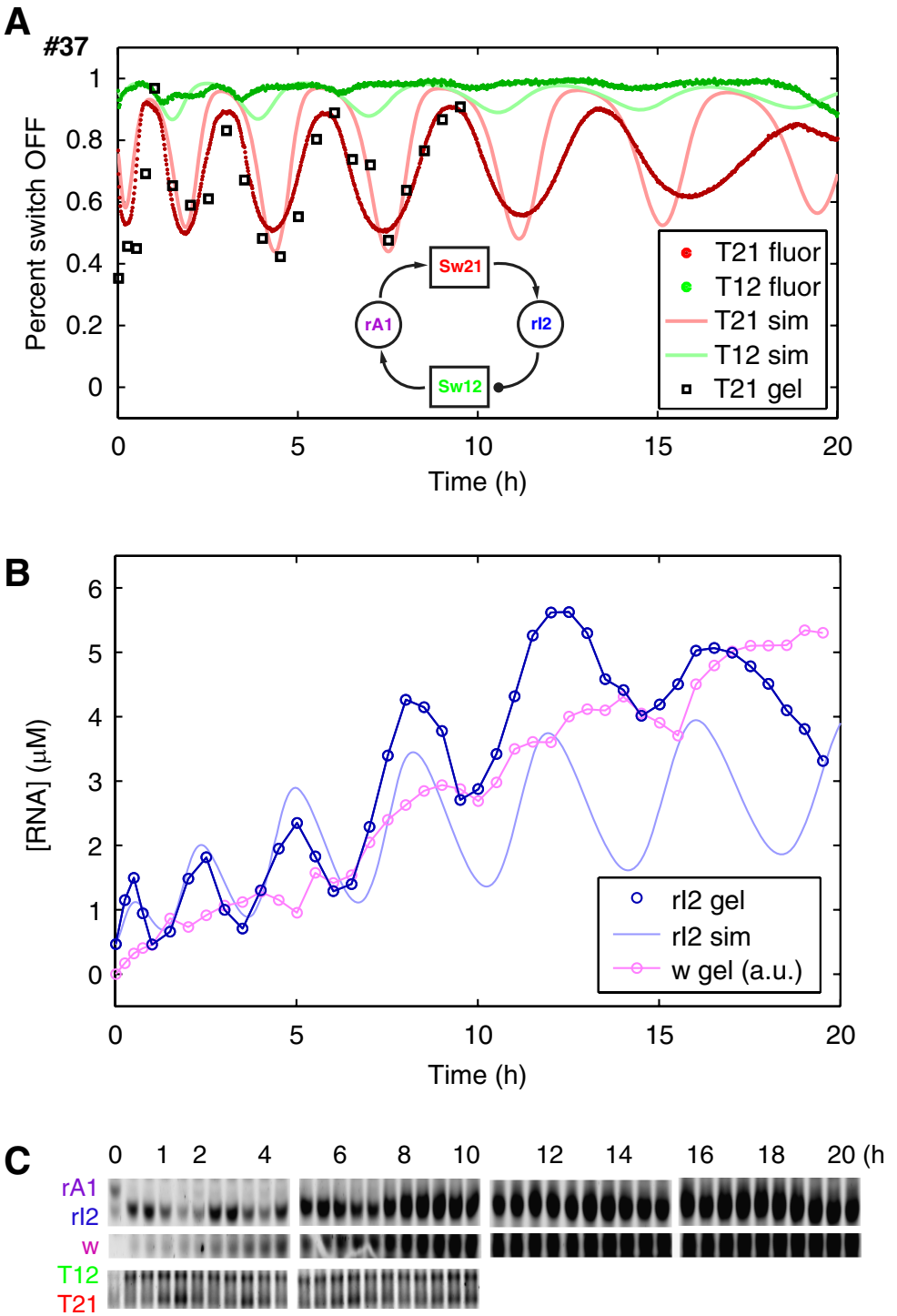

Jongmin Kim and Erik Winfree, Synthetic in vitro transcriptional oscillators, Molecular Systems Biology 7; Article number 465;

Error-correction in Strand displacement circuits of Dynamical systems (e.g., oscillators)

Rajiv Teja Nagipogu, John H. Reif,

[Accepted to Royal Society Interface]

(Used Shadow cancellation in conjunction to DNA Strand Displacement to reduce leakage errors)
(Simulations only)

Accepted paper to Royal Society Interface Journal

INTERFACE

rsif.royalsocietypublishing.org

Research

Article submitted to journal

Subject Areas:
DNA Computing, Molecular computing

Keywords:
DNA strand displacement, Leaks, Shadow cancellation, Dynamical systems

Author for correspondence:
Corresponding author
e-mail: rajivteja.nagipogu@duke.edu

Leak-resilient Enzyme-free Nucleic Acid Dynamical Systems through Shadow Cancellation

Rajiv Teja Nagipogu[1], John H. Reif[1]

[1]Department of Computer Science, Duke University, Durham, NC 27708, United States

DNA strand displacement is a prominent reaction motif that enables the construction of nucleic-acid computational devices that exhibit programmable behaviors. However, these circuits routinely suffer from background noise known as leaks. The side effects of such interactions are particularly severe in circuits with dynamical elements, as leaks could undergo exponential amplification, causing the circuit behavior to deteriorate rapidly. To tackle the leaks in such circuits, our group has previously introduced a dynamic technique known as "shadow cancellation". However, the method was conjectured to entail significant design overheads, which affected its use in practice. In this work, we use domain-level DSD simulations to examine more rigorously the method's capabilities, its inner workings, and, most importantly, its robustness to practical deviations in its design requirements. First, we show that the method could be extended to more complex catalytic and autocatalytic dynamical systems of practical importance. Then, using several probing experiments, we show that through simple adjustments to circuit parameters, its design restrictions could be significantly relaxed without significantly affecting the circuit dynamics. Finally, we discuss several design challenges and hint at ways to overcome them using the current capabilities of DNA nanotechnology, paving the way for future experimental work.

Background: React-Produce framework (Srinivas et al.)

CRN: U + V → X + Y

DNA Compressed: Ui + Vj → Xn + Yo

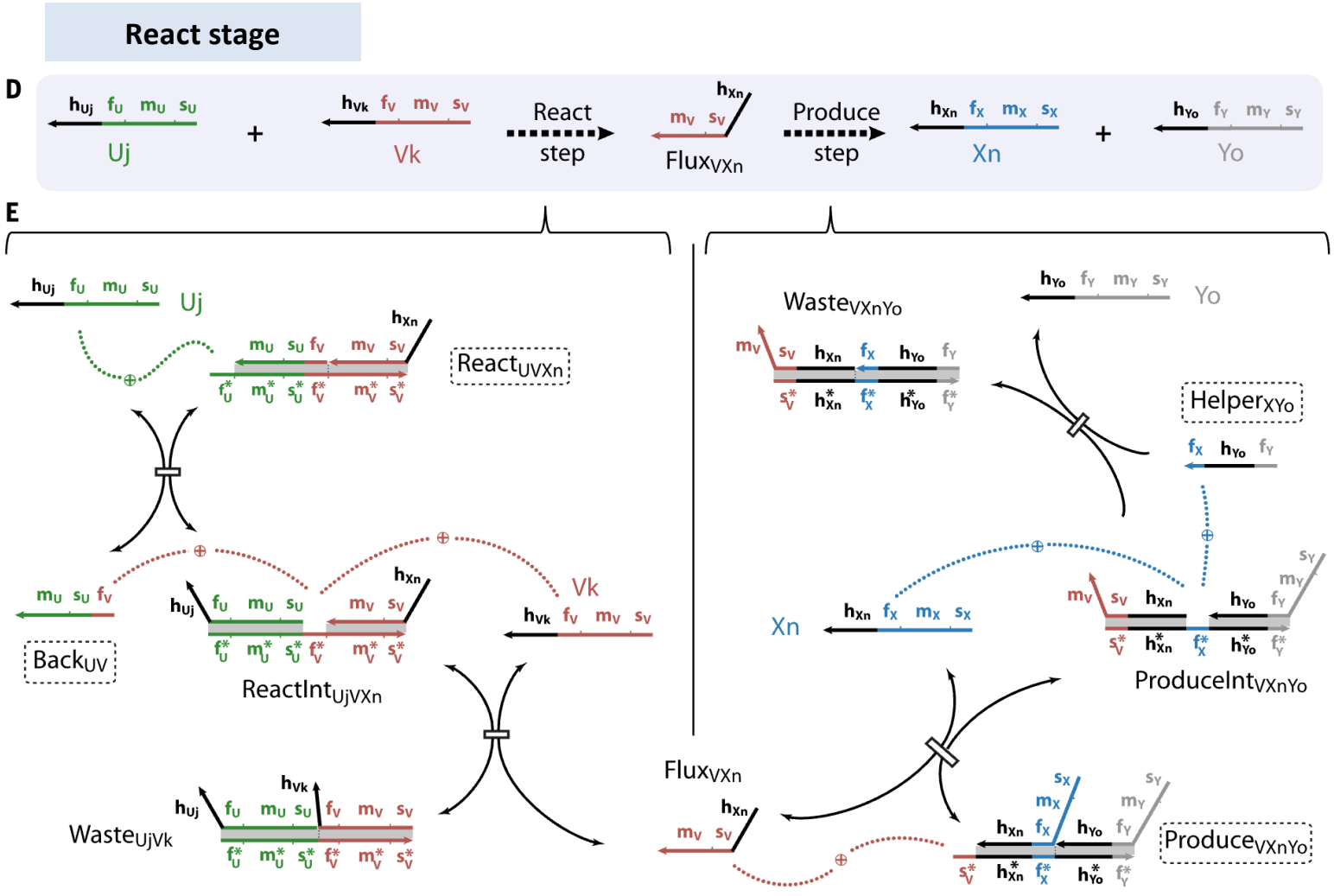

- Divides each reaction into 2 stages
  - React
  - Produce
- **React:** Reactants consumed
- **Produce:** Product released

Background: Fraying at the helix ends

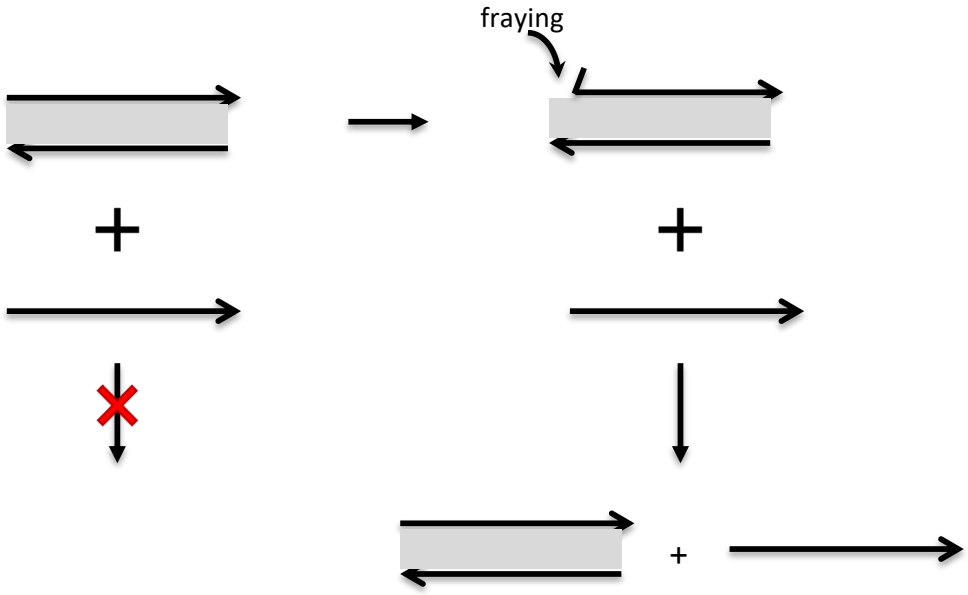

- I: No toehold ➔ No reaction

- II: Nucleotides at helix ends spontaneously dissociate
- Opens-up a short toehold
- Results in unexpected products

[Background] Leak pathways in React-Produce framework

React-second input leak:

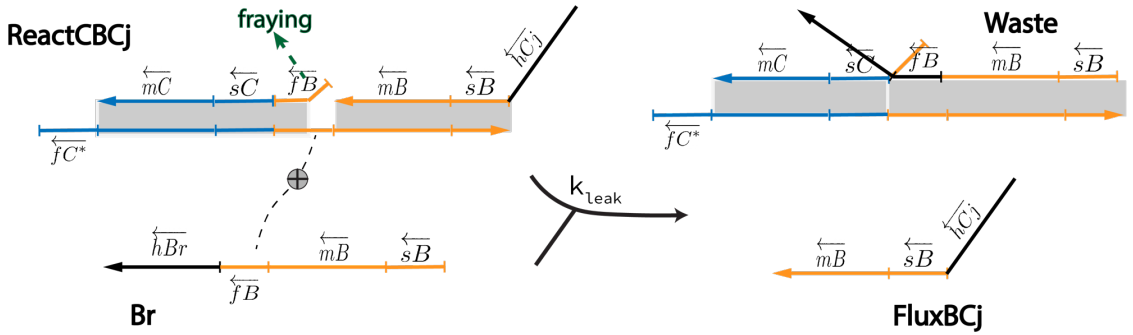

React-Produce leak:

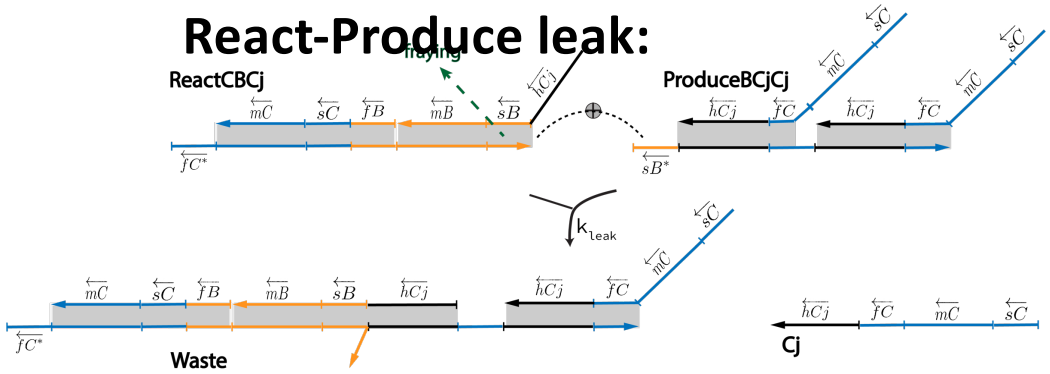

Produce-Helper leak

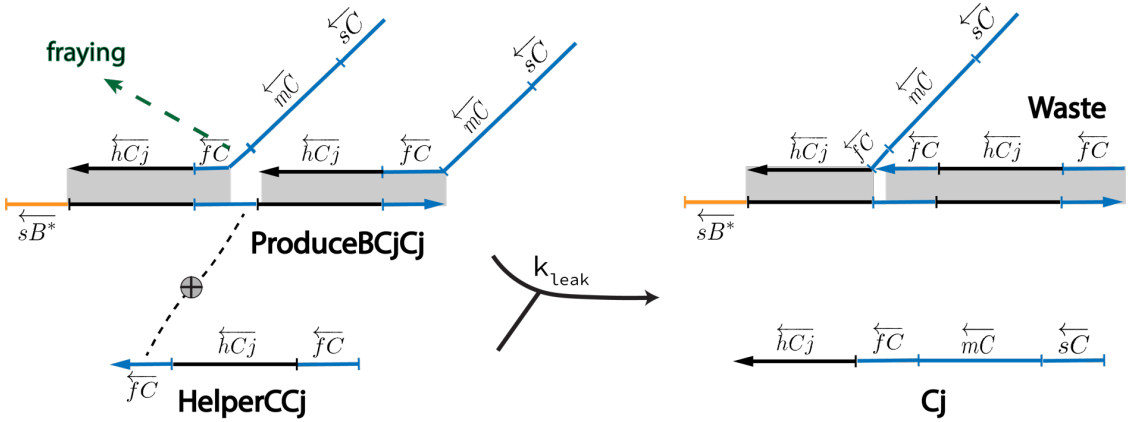

- Produce-Helper leak is dominant
  - Two fuel species

[Background] Effects of leaks in oscillatory circuits

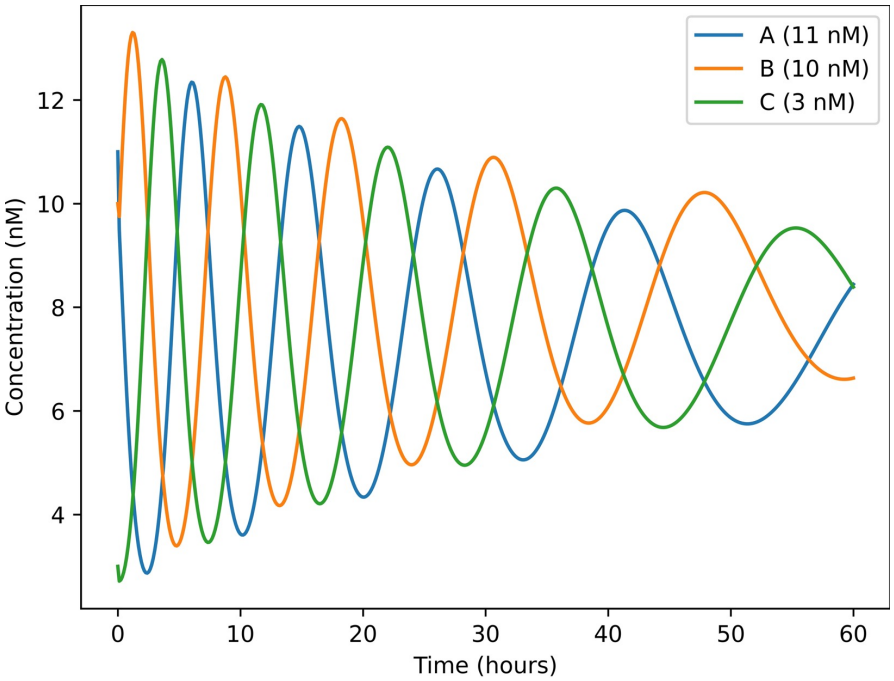

Dynamics w/o leaks

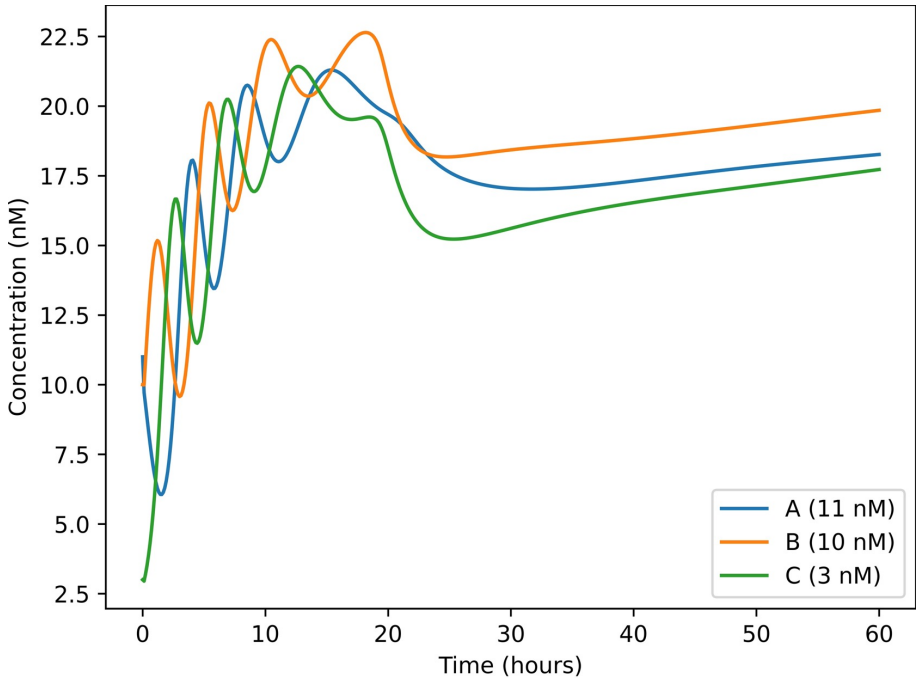

Dynamics w/ leaks

- **The ill-effects of leaks are especially severe in autocatalytic circuits**
- **A small amount of leak can uncontrollably amplify, degrading the circuit**

[Background] Shadow cancellation

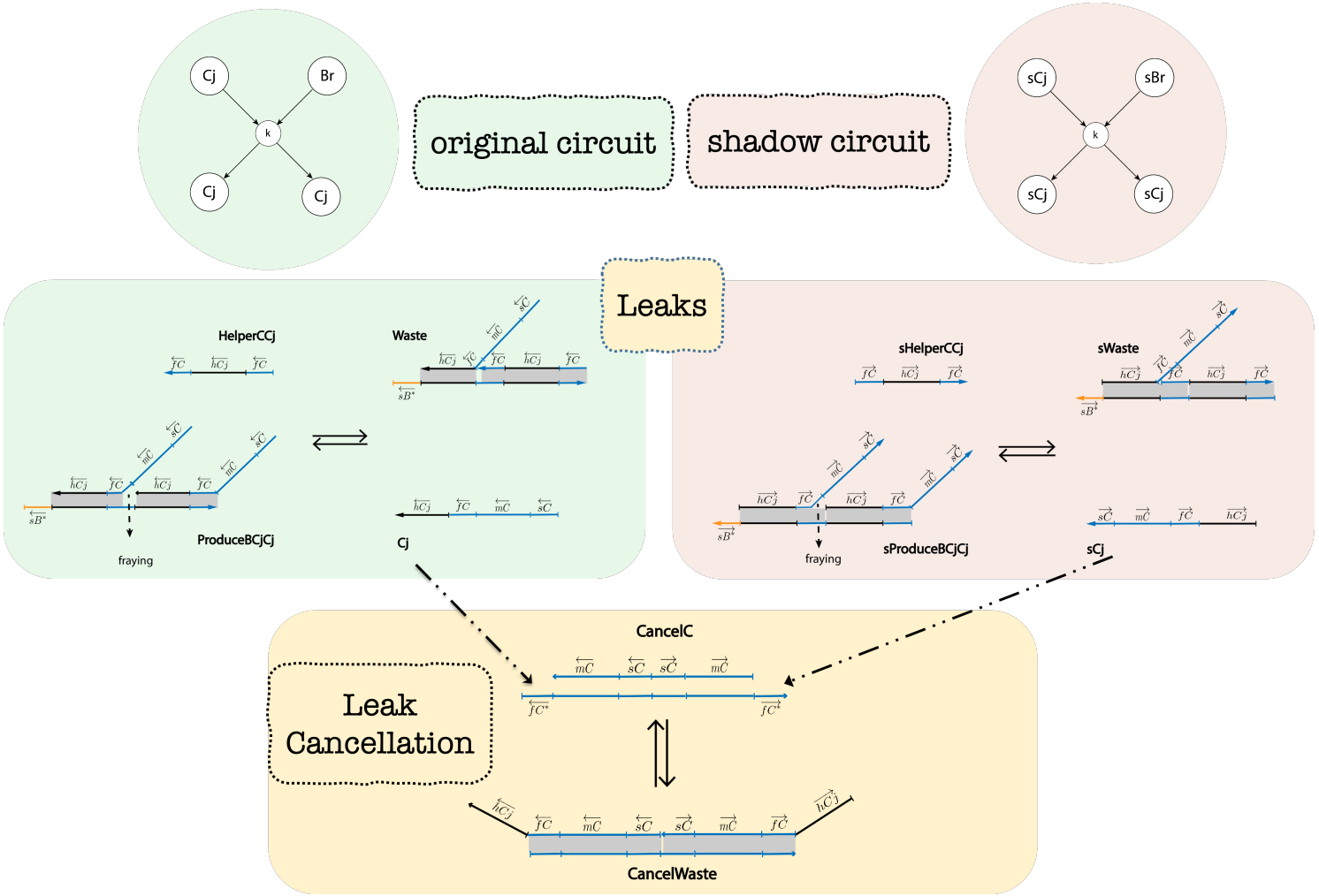

- An orthogonal "shadow" circuit
- Leak activity like the primary circuit
- Leaks from two circui are conjunctively sequestered
- Cooperative hybridization complexes

[Results] Shadow cancellation improves the kinetics of autocatalytic circuits

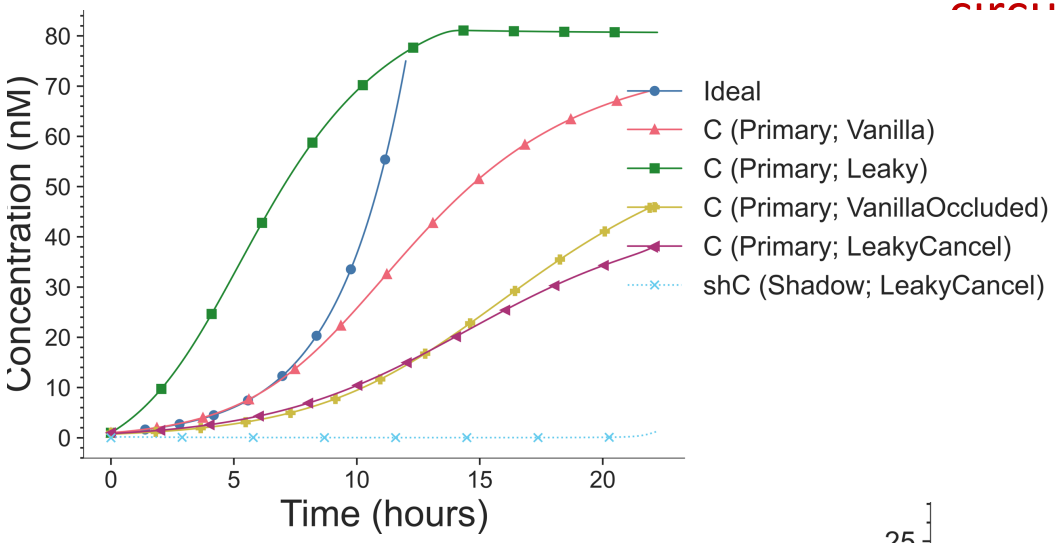

Unimolecular autocatalytic amplifier

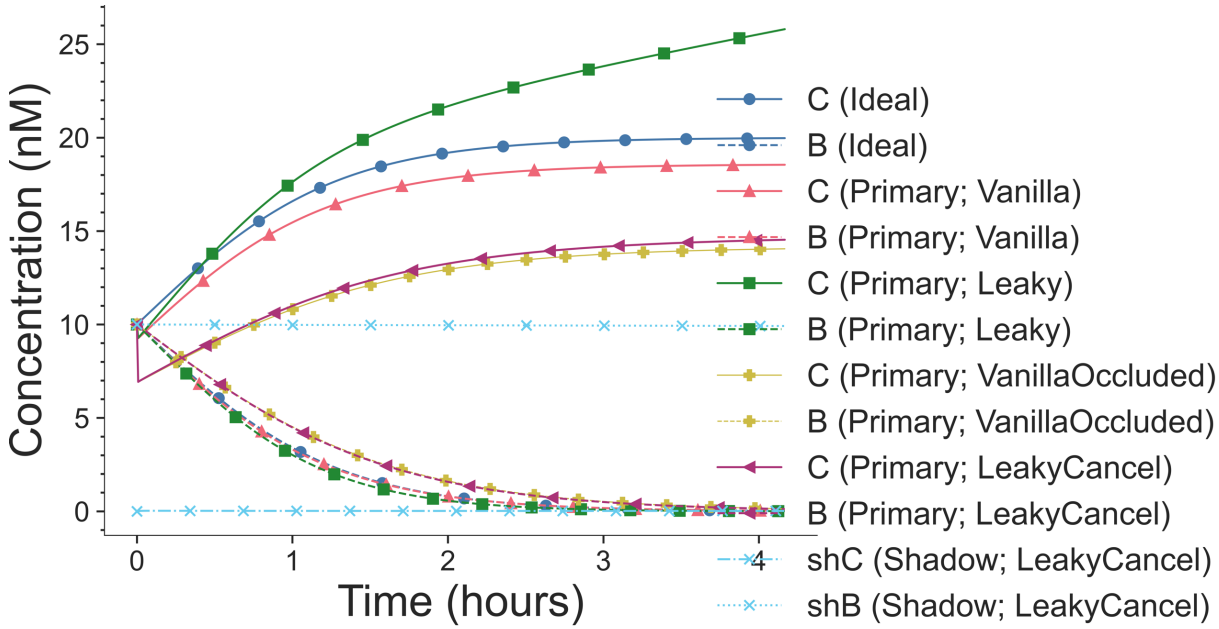

Bimolecular autocatalytic amplifier

[Results] Rock-Paper-Scissors oscillator circuit

Rock-Paper-Scissors oscillator

A

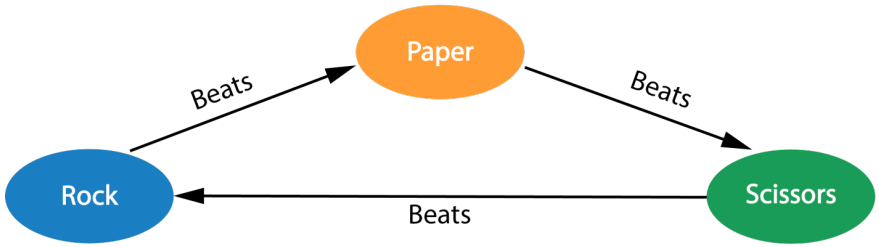

B

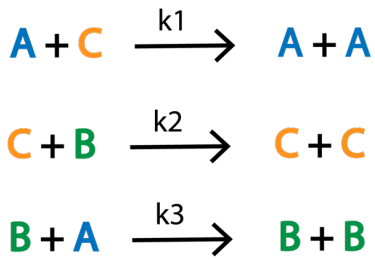

C

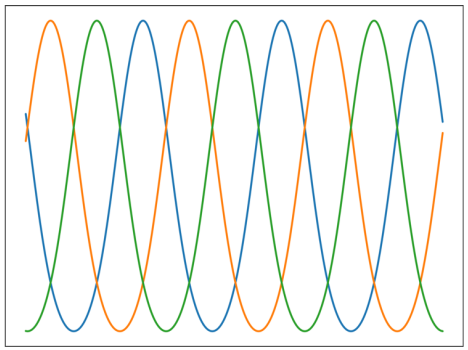

No Buffering

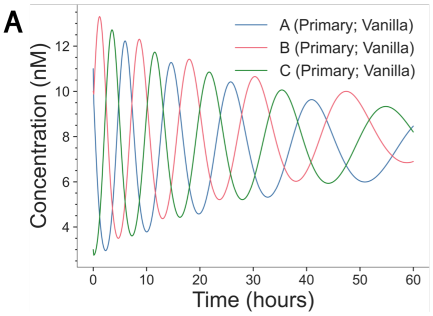

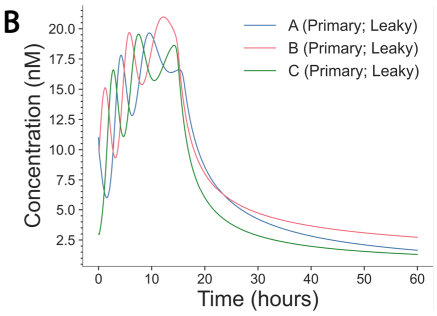

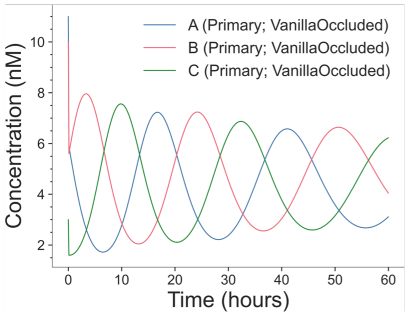

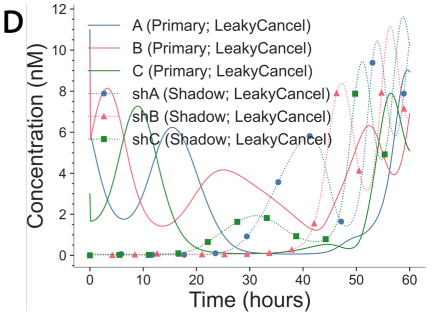

Buffering

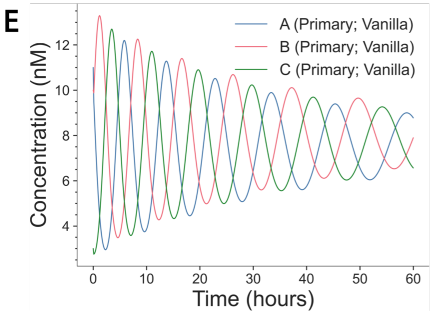

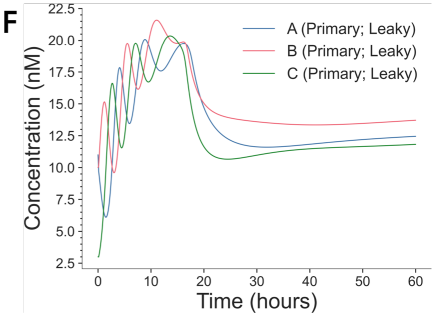

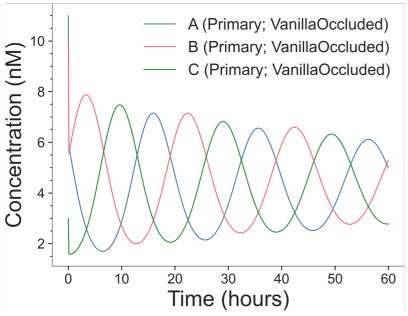

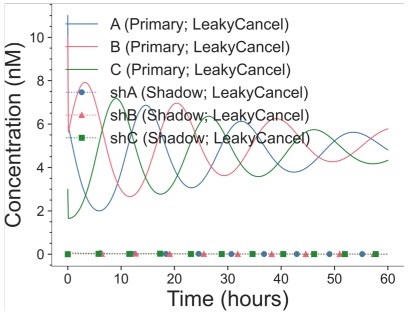

[Results] Consensus protocol

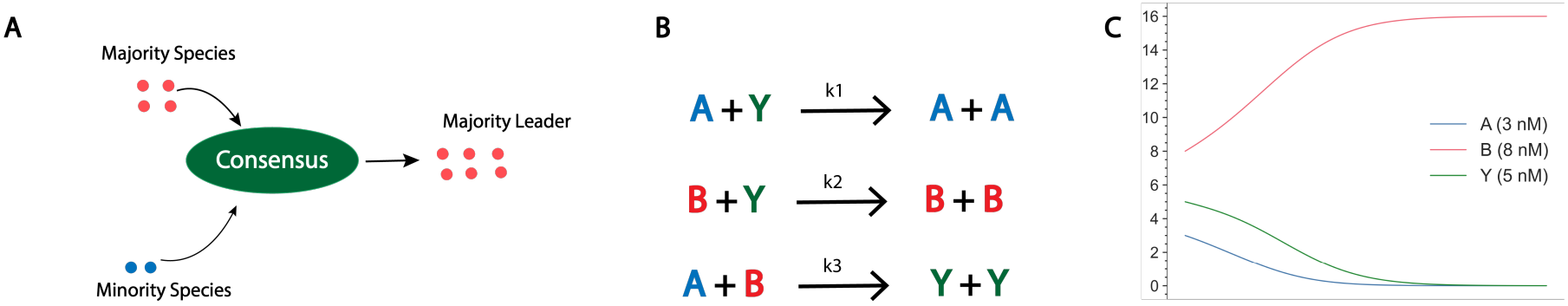

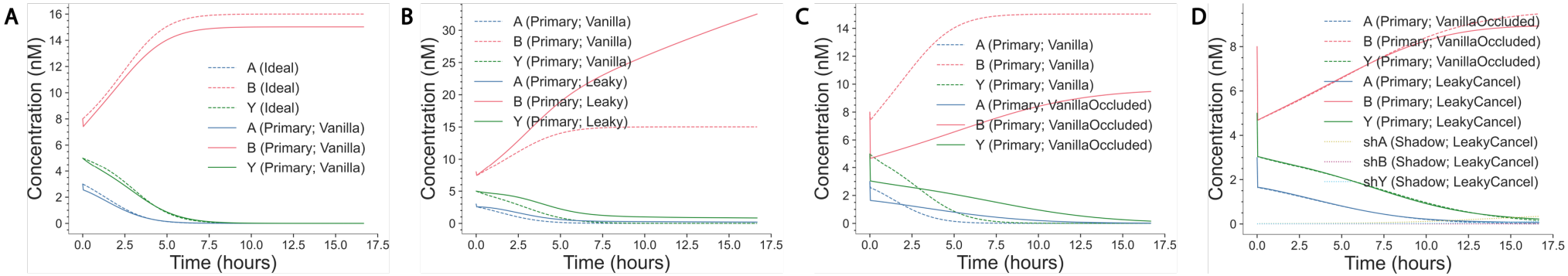

Two-molecule Consensus protocol

[Results] Feedback controller circuit

Proportional Integral feedback controller

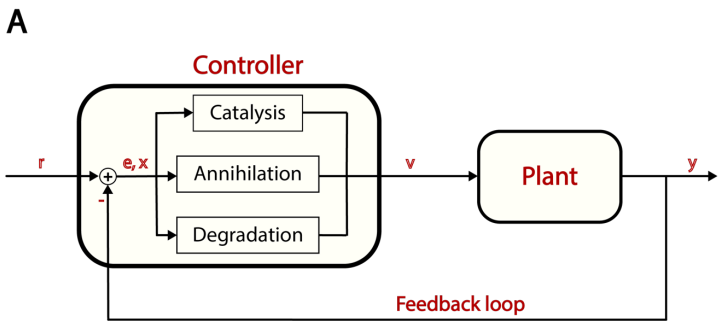

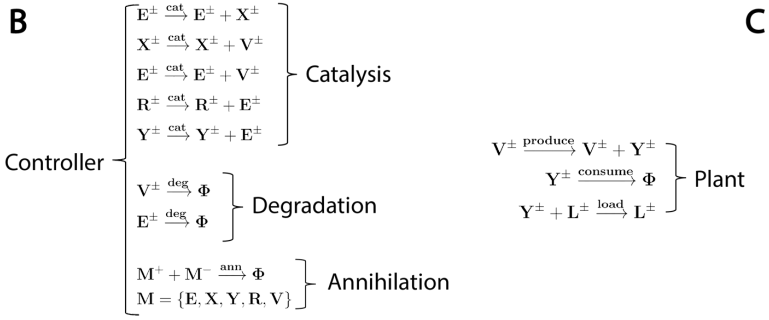

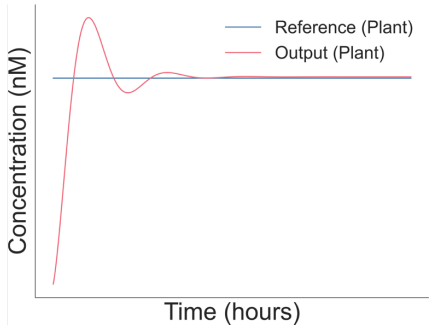

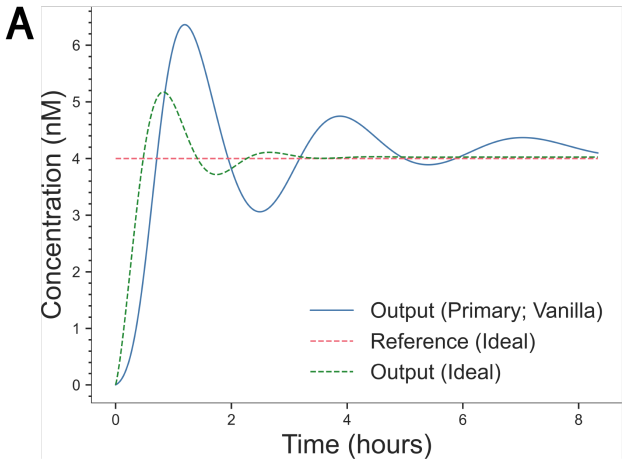

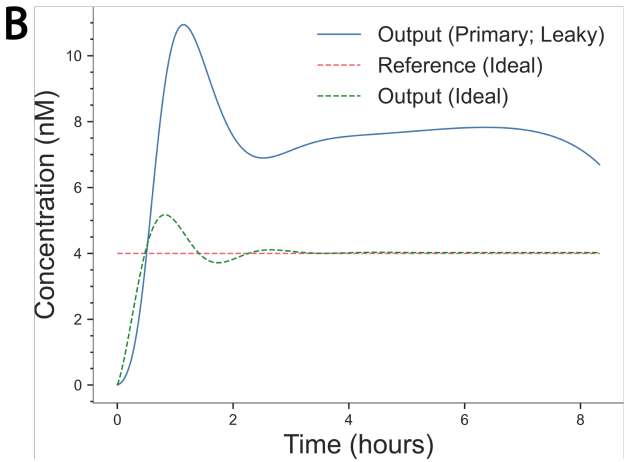

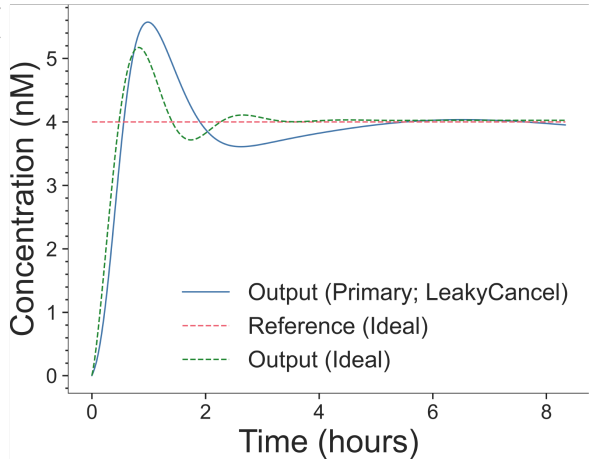

[Results] Shadow cancellation is robust to differences in the rates of primary and shadow circuit

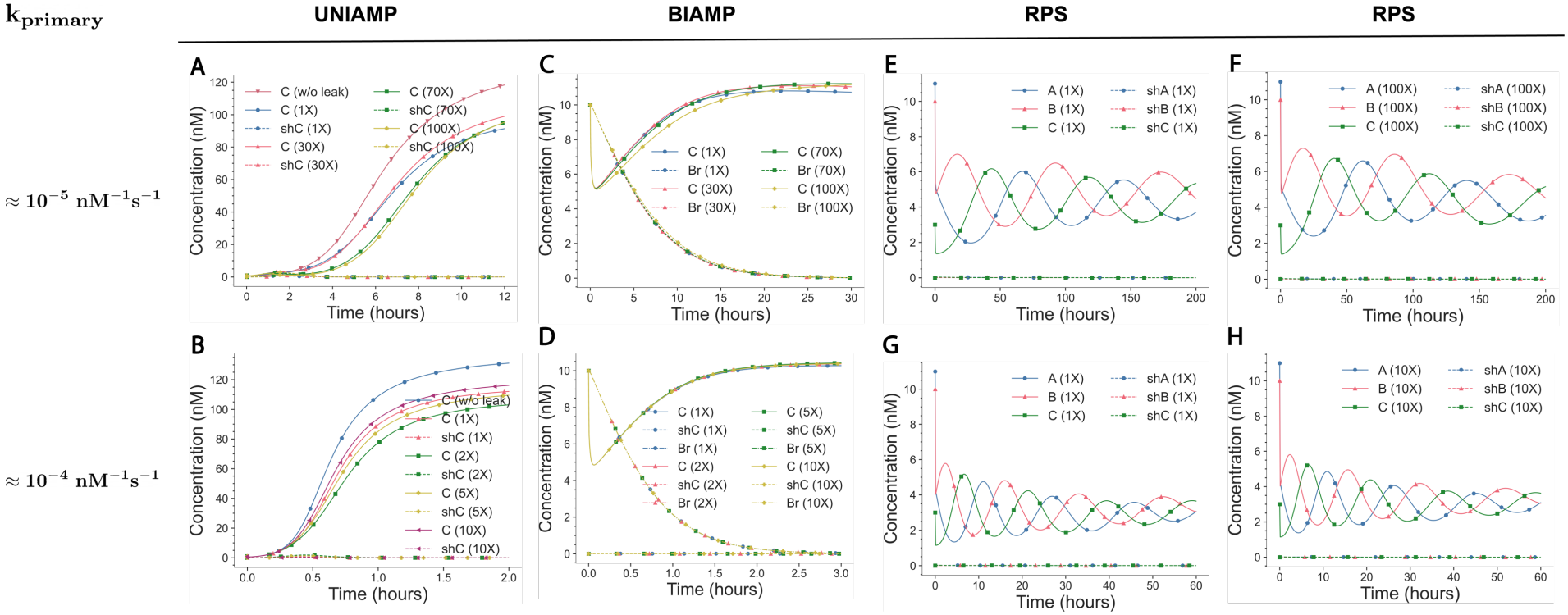

- The $k_{primary}$ are frozen; k_{shadow} are scaled up until $100X$
- The concentrations of the shadow circuit are scaled down appropriately
- Even at $100X$ perturbation, the circuit works fine.

$$[Fuel]_{new} = \frac{[Fuel]_{old}}{p^{SCALE}}, \qquad p = \frac{k_{shadow}}{k_{primary}}$$

The method previously required that the two circuits should run with the same rate

[Results] Shadow cancellation is robust to differences in the leak rates of primary and shadow circuit

$$\Delta Leak = \frac{k_{leak}^{shadow} - k_{leak}^{primary}}{k_{leak}^{primary}} * 100$$

- **Circuits stay stable even when the leak rate constants are at either extremes of the possible range.**

UNIAMP

BIAMP

RPS (same leak rates)

RPS (700% difference in leak rates)

A

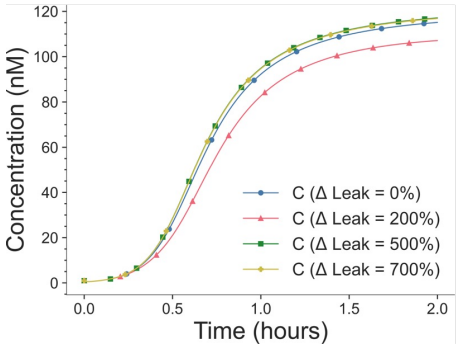

B

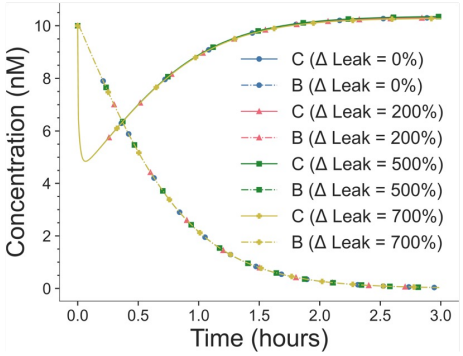

C

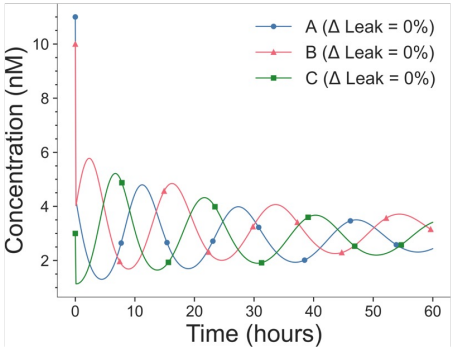

D

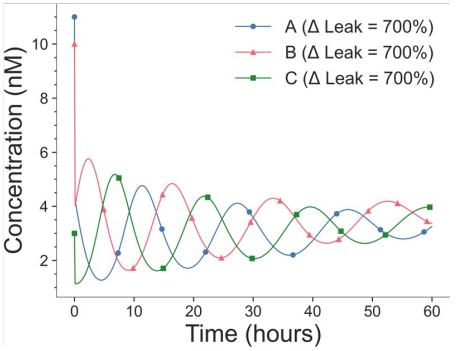

- **Residual leak left in the circuit after cancellation – close to zero**
- **Similar amount of cancellation complexes consumed – similar amount of leak generated**